

DEVELOPMENT OF THE POLY (2-ETHYL-2-OXAZOLINE) (PETOX) BASED
MULTIFUNCTIONAL CARRIER SYSTEMS FOR TREATMENT AND DIAGNOSIS
OF PROSTATE CANCER

by
Polen Koçak

Submitted to Graduate School of Natural and Applied Sciences
in Partial Fulfillment of the Requirements
for the Degree of Master of Science in
Biotechnology

Yeditepe University

2017

DEVELOPMENT OF THE POLY (2-ETHYL-2-OXAZOLINE) (PETOX) BASED
MULTIFUNCTIONAL CARRIER SYSTEMS FOR TREATMENT AND DIAGNOSIS
OF PROSTATE CANCER

APPROVED BY:

Assoc. Prof. Dr. Dilek Telci
(Thesis Supervisor)



Assoc. Prof. Dr. Elif Damla Arısan



Assist. Prof. Dr. Hüseyin Çimen



DATE OF APPROVAL:/....../2017

ACKNOWLEDGEMENTS

First of all, I would like to express my gratitude to my supervisor, Assoc. Prof. DILEK TELCI for her support, guidance and encouragement. I also want to thank Prof. Dr. Fikretin Şahin who inspired me for being a scientist.

I am deeply thankful to TUBITAK for supporting this work with 213M726 project entitled as ‘Development of The Poly (2-Ethyl-2-Oxazoline) (Petox) Based Multifunctional Carrier Systems for Treatment and Diagnosis of Prostate Cancer’’. I also want to thank to my thesis jury members, Assist. Prof. Hüseyin Çimen and Assoc. Prof. Damla Arısan for their support and attention.

I am so thankful to my best friends, Burge Ulukan, Merve Yıldırım, Melis Kalkan, Aycan Akay and Sevinc Gedik for their understanding and endless patience during this thesis. I want to thank especially to Burge Ulukan for being there for me when I needed.

I also want to thank my lab mates; Zeynep, Hande, Inci, Ayca, Halime, Dilara, Tarık, and Elif for their support and encouragement.

Finally, my deepest thanks go to my family, Sevilay Koçak, Mehmet Koçak and my one and only, Doğuş Koçak and lastly, I owe my loving thanks to my soul mate, Yağız Denizci and Deniz Denizci.

To all, I really thank you for your support and guidance, either morally, financially and physically.

ABSTRACT

DEVELOPMENT OF THE POLY (2-ETHYL-2-OXAZOLINE) (PETOX) BASED MULTIFUNCTIONAL CARRIER SYSTEMS FOR TREATMENT AND DIAGNOSIS OF PROSTATE CANCER

Prostate cancer is the second most frequently diagnosed cancer which is about 15-20% of all male cancers worldwide. Combination therapy methods ensure successful results when radiotherapy, chemotherapy or surgery alone is mostly unsuccessful. Prostate cancer is characterized by high the expression levels of prostate membrane specific antigen (PMSA), which made this membrane antigen to be used in the targeted therapies. For this purpose, this study aims to develop a new approach to specifically target prostate cancer using new generation nanocarriers delivering a pro-apoptotic gene, which has not been used in the treatment of prostate cancer before. The transfection of pro-apoptotic gene BIKDDA to PMSA-positive prostate cancer cell line 22RV1 using with X-tremeGENE HP transfection reagent potentiated a significantly higher cell death in comparison to the level induced by TRAIL expression. The treatment of 22RV1 and healthy human cell lines poly (2-ethyl-2-oxazoline-co-ethylenimine) (PEtOx-co-PEI) PetOx5900-b-PCL4200 polymer and its functionalized polymersome showed no toxicity. Treatment of 22RV1 cells with PetOx5900-b-PCL4200 polymersome encapsulated BIKDDA (PSm-BIKDDA) gene led to an increased apoptotic potential when compared to with X-tremeGENE HP suggesting that once targeted PetOx5900-b-PCL4200 polymersome could be useful as delivery systems. Initial work from this thesis suggested that peptide 563 (GRFLTGGTGRLLRIS) successfully targeted PMSA positive 22RV1 as the healthy control HUVEC and PNT1A cells were found to be poor targets for this peptide. Data from this thesis suggests that P563-targeted PetOx5900-b-PCL4200 polymersome delivering pro-apoptotic gene BIKDAA could be a useful therapeutic option in prostate cancer treatment.

ÖZET

PROSTAT KANSERİ TEŞHİS VE TEDAVİSİNDE KULLANILACAK POLİ(2ETİL-2OKSAZOLİN) PETOKS ESASLI ÇOK İŞLEVSEL TAŞIYICI SİSTEMLERİN GELİŞTİRİLMESİ

Prostat kanseri, dünya çapında tüm erkek kanserlerinin yaklaşık yüzde 15-20'si arasında ikinci en sık teşhis edilen kanserdir. Tedavi yöntemlerini birleştirmek, radyoterapi, kemoterapi veya tek başına ameliyatın çoğunlukla başarısız olması durumunda başarılı sonuçlar verir. Prostat kanseri, prostat spesifik membran antijenini (PMSA) yüksek oranda ihtiva etmektedir ve bu sebeple prostat-spesifik membran antijeni, hedefleyici tedavi yöntemlerinde kullanılabilir. Bu amaçla, bu çalışma, daha önce prostat kanseri tedavisinde kullanılmamış, pro-apoptotik bir gen taşıyan yeni nesil nanotaşıyıcı kullanarak prostat kanserini spesifik olarak hedeflemeye yönelik yeni bir yaklaşım geliştirmeyi amaçlamaktadır. PMSA-pozitif prostat kanseri hücre hattı 22RV1, pro-apoptotik gen olarak kullanılan BIKDDA ve TRAIL ile X-tremeGENE HP transfeksiyon reaktifi kullanılarak transfekte edilmiş, BIKDDA transfeksiyonu yapılmış prostat kanseri hücrelerinde daha yüksek oranda hücre ölümü görülmüştür. 22RV1 ve sağlıklı insan hücrelerinin poli (2-etil-2-oksazolin-co-etilenimin) (PEtOx-co-PEI) PetOx5900-b-PCL4200 polimeri ve formülasyonu ile muamelesinde her hangi bir toksik etki görülmemiştir. BIKDDA geni aktarımında PetOx5900-b-PCL4200 polimerzomunun kullanılması X-tremeGENE HP ile karşılaştırıldığında daha yüksek seviyede gen ifadesine ve dolayısı ile hücre ölümüne yol açmıştır. Elde ettiğimiz bu sonuç hedeflenen PetOx5900-b-PCL4200 polimerzomunun taşıyıcı sistem olarak kullanımının yararlı olabileceğini düşündürmektedir. Hedefleme üzerine yaptığımız deneyler, peptit 563'ün (GRFLTGGTGRLLRIS), PMSA pozitif 22RV1'i başarıyla hedeflediğini, bunun yanı sıra sağlıklı kontrol olan HUVEC ve PNT1A hücrelerinin bu peptit için zayıf hedefleyici etkisi olduğunu önermiştir. Bu tezin verileri, pro-apoptotik gen BIKDDA taşıyan ve P563 hedeflenen PetOx5900-b-PCL4200 polimerzomunun prostat kanseri tedavisinde yararlı bir terapötik seçenek olabileceğini düşündürmektedir.

TABLE OF CONTENTS

ACKNOWLEDGEMENTS	iii
ABSTRACT	iv
ÖZET	v
LIST OF FIGURES	ix
LIST OF TABLES	xii
LIST OF SYMBOLS/ABBREVIATIONS	xiii
1. INTRODUCTION	1
1.1. ANATOMY AND PHYSIOLOGY OF THE PROSTATE.....	1
1.2. PROSTATE CANCER.....	3
1.3. EPIDEMIOLOGY OF PROSTATE CANCER.....	3
1.4. PATHOLOGICAL STAGES OF PROSTATE CANCER.....	5
1.4.1. TNM Classification System	5
1.4.2. Gleason Score	5
1.5. MOLECULAR MECHANISMS IN THE DEVELOPMENT OF PROSTATE CANCER.....	6
1.5.1. PI3K/Akt Signaling Pathway and PTEN in Prostate Cancer	7
1.6. ANDROGEN RECEPTORS IN PROSTATE CANCER	9
1.7. PROGNOSTIC SIGNIFICANCE OF INSULIN-LIKE GROWTH FACTOR-I RECEPTOR (IGFIR) EXPRESSION IN PROSTATE CANCER CELL DEATH MECHANISMS	11
1.8. VASCULAR ENDOTHELIAL GROWTH FACTOR IN PROSTATIC CANCER THERAPY STRATEGIES FOR PROSTATE CANCER	12
1.9. CELL DEATH MECHANISMS.....	13
1.10. THERAPY STRATEGIES OF PROSTATE CANCER	16
1.11. TARGETED THERAPIES FOR PROSTATE CANCER	17
1.12. THE AIM OF THE STUDY.....	19
2. MATERIALS.....	20
2.1. INSTRUMENTS	20
2.2. EQUIPMENTS	20
2.3. CHEMICALS	21
2.3.1. Cell Culture Media	21

2.3.2. Growth Supplements	21
2.3.3. Other Reagents	22
2.4. KITS AND SOLUTIONS.....	23
2.5. ANTIBODIES	23
2.5.1. Primary Antibodies.....	23
2.5.2. Secondary Antibodies.....	23
2.6. CELL LINES	24
3. METHODS	25
3.1. CELL CULTURE METHODS.....	25
3.1.1. Cell Types and Culturing Conditions	25
3.1.2. Cell Passaging	25
3.1.3. Determination of Cell Number	26
3.1.4. Cell Cryopreservation.....	26
3.1.5. Cell Thawing	26
3.2. SYNTHESIS AND CHARACTERIZATION OF BIKDDA PLASMID	27
3.2.1. Plasmid Construction and Site-directed Mutagenesis	27
3.2.2. Plasmid Isolation	29
3.3. PLASMID DNA TRANSFECTION	30
3.3.1. Determination of Transfection Efficiency.....	30
3.4. DETECTION of GENE EXPRESSION LEVELS of TRAIL and BIKDDA in 22RV1 CELL LINE	31
3.4.1. RNA Isolation.....	31
3.4.2. Reverse Transcriptase Polymerase Chain Reaction	31
3.4.3. Quantitative Polymerase Chain Reaction.....	32
3.5. MEASUREMENT OF PROTEIN LEVELS IN 22RV1 CELL LINE	33
3.5.1. Total Cell Lysate Preparation.....	33
3.5.2. Lowry Assay.....	34
3.5.3. Sodium Dodecyl Sulfate-Polyacrylamide Gel Electrophoresis (SDS- PAGE).....	34
3.5.4. Western Blotting.....	35
3.6. SYNTHESIS AND CHARACTERIZATION OF PEPTIDES TARGETING PROSTATE CANCER.....	36
3.6.1. Synthesis of Peptides.....	36

3.6.2. Determination of Peptide Binding Affinity by Flow Cytometry.....	36
3.6.3. Determination of Peptide Binding Affinity by Confocal Microscope	37
3.7. DETERMINATION OF CELL DEATH.....	37
3.7.1. Trypan Blue	37
3.7.2. Annexin V	38
3.8. THE CYTOTOXICITY OF NANOCARRIERS.....	38
4. RESULTS	39
4.1. SITE DIRECTED MUTAGENESIS OF BIKDD TO BIKDDA	39
4.2. DETERMINATION OF THE TRANSFECTION EFFICENCY OF TRAIL AND BIKDDA ON 22RV1 CELLS USING EXTREME GENE TRANSFECTION REAGENT.....	41
4.3. GENE EXPRESSION LEVEL OF BIKDDA AND TRAIL IN 22RV1 CELL LINE.....	43
4.4. PROTEIN EXPRESSION LEVEL OF BIKDDA AND TRAIL IN 22RV1 CELL LINE.....	45
4.5. EFFECT OF PRO-APOPTOTIC GENE TRANSFECTION ON THE CELL VIABILITY	46
4.6. DETERMINATION OF APOPTOSIS BY ANNEXIN V	47
4.7. THE CYTOTOXICITY OF NANOCARRIERS.....	49
4.8. POLYMERSOME DELIVERY OF BIKDDA TO 22RV1 CELLS	54
4.9. BINDING AFFINITY OF PEPTIDE 562, PEPTIDE 563, AND PEPTIDE 564 TO PROSTATE CANCER AND HEALTHY CONTROL CELL LINES.....	56
4.10. DETERMINATION OF BINDING AFFINITY OF PEPTIDES BY CONFOCAL MICROSCOPY	58
5. DISCUSSION.....	60
6. FUTURE PROSPECTS.....	63
REFERENCES	64

LIST OF FIGURES

Figure 1.1. The Prostate Anatomy and Physiology	2
Figure 1.2. The prostate cancer incidence and mortality rates between 1998-2002.....	4
Figure 1.3. Histological grades of Prostate Cancer according to the Gleason Grading System.....	6
Figure 1.4. PI3K/Akt/mTOR Pathway.....	8
Figure 1.5. The Mechanism of the Androgen Receptor.....	11
Figure 1.6. The Intrinsic and Extrinsic pathway of Apoptosis.	15
Figure 3.1. Colony formation of BIKDDA transformed with XL-ultra competent cells after 16 hours.....	29
Figure 3.2. Colony formation of control petri plates after 16 hours	29
Figure 4.1. The Chromatogram result of the site directed mutagenesis	40
Figure 4.2. 22RV1 cells were transfected with pEGFP-BIKDDA by X-tremeGENE HP DNA transcription reagent using 1:1, 1:2 and 1:3 ratios of DNA:Transfection reagent ratio	41
Figure 4.3. 22RV1 cells were transfected with pEGFP-TRAIL by X-tremeGENE HP DNA transcription reagent using 1:1, 1:2 and 1:3 ratios of DNA:Transfection reagent ratio.	42
Figure 4.4. BIK mRNA levels were analyzed using qPCR in BikDDA transfected and non-transfected (Cnt) 22rv1 cells.....	44

Figure 4.5. TRAIL transfected and untreated (Cnt) 22rv1 cells was evaluated using Qpcr....	45
Figure 4.6. Western Blot analysis proteins in non-transfected (CNT), (A) Bik and (B) TRAIL transfected, and mock vector transfected (pEGF-c3) 22RV1 Cell Lines.....	46
Figure 4.7. Effect of Pro-apoptotic gene transfection on the cell viability of 22RV1 cells. A trypan blue assay was then used to measure cell viability.....	47
Figure 4.8. The Annexin V staining on BIKDDA transfected 22rv1 cells.....	48
Figure 4.9. The cytotoxic efficacy of A. PetOx5900-b-PCL4200 polymer and B. PetOx5900-b-PCL4200 polymersome formulation on the primary human dermal fibroblast cells (HDF).....	50
Figure 4.10. The cytotoxic efficacy of A. PetOx5900-b-PCL4200 polymer and B. PetOx5900-b-PCL4200 polymersome formulation on the healthy prostate epithelium immortalized cell line PNT1A.....	51
Figure 4.11. The cytotoxic efficacy of A. PetOx5900-b-PCL4200 polymer and B. PetOx5900-b-PCL4200 polymersome formulation on the healthy liver hepatocellular cell line HEPG2.....	52
Figure 4.12. The cytotoxic efficacy of A. PetOx5900-b-PCL4200 polymer and B. PetOx5900-b-PCL4200 polymersome formulation on the human fetal osteoblastic cell line Hfob 1.19.....	53
Figure 4.13. 22RV1 cells were incubated with PSm-BIKDDA for 24 hours.....	54
Figure 4.14. Polymersome encapsulated BIKDDA transfected and untreated (Cnt) 22rv1 cells was evaluated using qPCR.....	55

Figure 4.15. Annexin V staining of 22RV1 cells treated with PSm-BIKDDA polymersome.....	56
Figure 4.16. Representative histograms showing the binding activity of peptide 562 (P562), peptide 563 (P563) and peptide 564 (P564) to 22RV1, PNT1A and HUVEC.....	57
Figure 4.17. Peptide binding Affinity on A. PNT1A cell line B. 22RV1 cell line by confocal microscopy.....	59

LIST OF TABLES

Table 3.1. PCR Components for Site-Directed Mutagenesis	27
Table 3.2. PCR Conditions	28
Table 3.3. RT PCR Reaction Master Mix.....	32
Table 3.4. Quantitative PCR Conditions.....	33
Table 3.5. The ingredients of Stacking And Separating Gel	34
Table 3.6. The Sequence of the Peptides	36
Table 4.16. Average Percentage of Binding Affinity Recorded for the Targeting Peptides onto PNT1A, 22RV1 and HUVEC Cells.....	56

LIST OF SYMBOLS/ABBREVIATIONS

AIF	Apoptosis stimulating factor
AKT	Protein kinase B
APS	Ammonium persulfate
AR	Androgen receptor
ATTC	American type culture collection
BPH	Benign prostatic hyperplasia
BSA	Bovine serum albumin
cDNA	Complementary deoxyribonucleic acid
DHT	Dihydrotestosterone
DMEM	Dulbecco's modified Eagle's medium
DMSO	Dimethyl sulfoxide
ECM	Extracellular matrix
EDTA	Ethylenediaminetetraacetic acid
EGF	Epidermal growth factor
EGFR	Epidermal growth factor receptor
ETR	Endothelin receptor
FBS	Fetal bovine serum
HSP	Heat shock protein
IGF1R	Insulin growth factor 1 receptor
IP3	Inositol triphosphate
M	Molar
ml	Milliliter
μ l	Microliters
mM	Millimolar
MEK	Mitogen-activated protein kinase
MTOR	Mammalian target of rapamycin
NR3C4	Nuclear receptor subfamily 3, group C, member 4
PCA	Prostate cancer
PSA	Prostate specific antigen

PDGF	Platelet derived growth factor
PDGFR	Platelet derived growth factor receptor
PH	Plexirin homology
pH	Negative log of hydrogen ion concentration
PI3K	Phosphoinositide 3-kinase
PIP2	Phosphatidylinositol (4,5) bisphosphate
PIP3	Phosphatidylinositol 3, 4, 5 triphosphate
PTEN	Protein tyrosine phosphatase and tensin homology
P/S	Penicillin, streptomycin
QPCR	Quantitative polymerase chain reaction
RT	Reverse transcriptase
RTK	Receptor tyrosine kinase
SDS-PAGE	Sodium dodecyl sulfate polyacrylamide gel electrophoresis
TEMED	N,N,N',N'- Tetramethylethylenediamine
TG	Transglutaminase
TNF	Tumor necrosis factor
TRAIL	TNF-related apoptosis-inducing ligand
VEGF	Vascular endothelial growth factor
VEGFR	Vascular endothelial growth factor receptor 1
WST-	Water soluble tetrazolium salt

1. INTRODUCTION

1.1 ANATOMY AND PHYSIOLOGY OF THE PROSTATE

Prostate (it means "protective, guardian") is a glandular walnut sized organ of the male reproductive system in most mammals, located in front of the rectum, below and out of the bladder. It lies in the human body below the urinary bladder (in animals correspondingly behind) and covers the initial part of the urethra up to the basin floor. [1] Prostate functions as a secondary bladder that receives the semen of the vas deferens, and transports mature sperm to urethra [2-3]

The prostate gland is responsible from the production of prostate specific antigen, fibrinogen, spermine, zinc, magnesium which gives a milky white appearance to semen, and enzymes such as acid phosphatases, prostate transglutaminase (in rodents, semen densified so as to generate a vaginal plug preventing the outflow of semen and copulation by another male. [4-5] Male hormones trigger the prostate gland formation in the developing fetus. The prostate continues to grow until the onset of adulthood and maintains its size as long as male hormones are produced. In the absence of the male hormones, the prostate gland cannot develop and reach to a normal size sometimes resulting in the regression of the gland. [6]

The prostate can be divided into several sections: (i) fibro muscular stroma; poster laterally extends and forms the capsule, (ii) the transition zone, near the verumontanum and per urethral glandular tissue where prostatic hyperplasia is seen, (iii) the central area surrounding the transition zone, (iv) peripheral or marginal zone from which 75 per cent of prostate cancer arises from. [2-7]

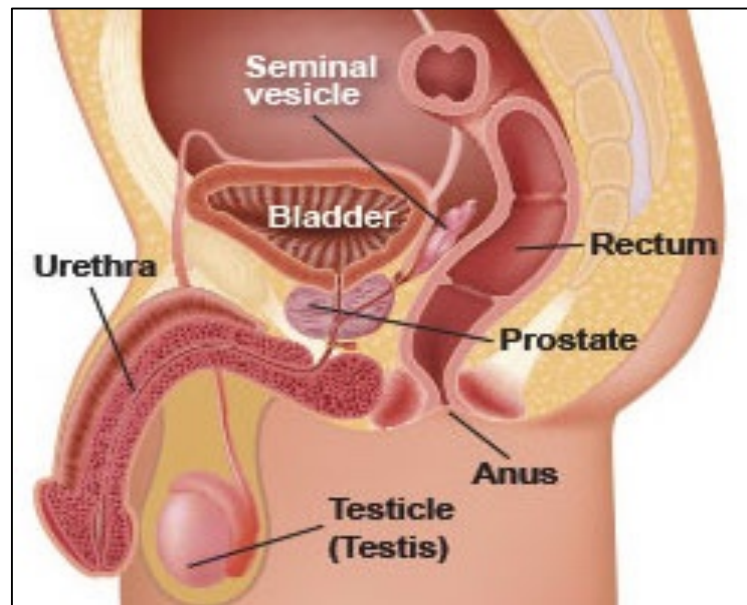


Figure 1.1. The prostate anatomy and physiology [7]

The most common diseases that arise from the prostate are prostatitis, benign prostatic hyperplasia, and prostate cancer. Prostatitis is the inflammation of the prostate, which may be infectious. Prostatitis can also produce symptoms of urinary tract infection but yields negative results in urine cultures. Acute prostatitis may be caused by sexually transmitted diseases, which often present with various symptoms such as fever. Chronic prostatitis tends to be prevalent in people over 50 years of age with large prostates or benign prostatic hypertrophy. Symptoms of prostatitis are usually unnoticed, and treatment requires long-term antibiotic intake. [8] Benign prostatic hyperplasia, known as BPH or prostate adenoma, is not cancer, but an organ growth (mostly in older men) termed as hypertrophy. It can cause symptoms of bladder irritation, urgency to urinate, decrease in urinary stream, or frequent urination, which is called prostatism. BPH has different complications, such as recurrent urinary tract infections, complete urinary retention, renal failure, hematuria, and bladder stones. [9] Prostate cancer is a very common disease of the prostate in men, majorly affecting the quality of life. In few cases, prostate cancer is aggressive. Depending on the stage of the tumor, treatments vary from surgery and radiation therapy with curative to palliative treatment such as hormone therapy and chemotherapy. [10]

1.2 PROSTATE CANCER

Prostate cancer (PCA) is a malignant tumor disease caused by the glandular tissue of the prostate gland. It occurs when prostate cells are transformed and begin to multiply uncontrollably. These transformed cells could also spread from the prostate to the other parts of the body, especially to the bones and the lymph nodes causing metastasis. Prostate cancer can spread to bladder, colon, lung, melanoma, lymphoma and other organs resulting in difficulty in urinating, erectile dysfunction, pain, and other symptoms. [11]

Prostate cancer occurs most often in people over 50 years and it is symptomless in the early stages. However, at an advanced stage, symptoms such as bladder dysfunction, bone pain, and later weight loss and blood loss may occur. If the diagnosis is made after the symptoms have already occurred, metastasis has already taken place primarily in the local lymph nodes or in the skeleton (bone metastases). [11] Various factors, including genetics and diet, have been implicated in the development of prostate cancer, but to date primary prevention modalities known are insufficient to eliminate the risk of contracting the disease. [12] Detection of prostate cancer is carried out mainly by the blood test measuring the levels of prostate-specific antigen or by the physical examination of the prostate gland called Digital Rectal Examination (DRE).

1.3 EPIDEMIOLOGY OF PROSTATE CANCER

Prostate cancer is the second most frequently diagnosed cancer which is about 15-20% of all male cancers in worldwide. Within the group of men who died of cancer, prostate cancer causes about seven per cent of deaths and thus represents the fourth most common lethal cancer after the lung, colorectal cancer and breast cancer. [19] The frequency of prostate cancer in the world countries is widely variable. The incidence of clinical prostate cancer varies among countries; The highest incidence is seen in the America, Western Europe and the Caribbean, while the lowest incidence is seen in Asian countries (Figure 1.2) [26]. This regional disparity suggests that environmental factors play an important role in prostate cancer risk factors. [20] According to the American Cancer Society, there are not only strong geographic differences in the frequency of prostate cancer but also the

ethnic background of males also plays an important role. In fact, prostate cancer is less common among Asian men, the most common among black men; the incidence among European men is intermediate compared to the previous two populations. [20-21] American Cancer Society 2016 report states that the annual incidence rate for prostate cancer in Central Asia is less than 3 / 100,000, while in the North American the incidence rate is more than 160 / 100,000. However, the detection of these higher frequencies may have been influenced by new regulations in the diagnostic progress and prevention policies [19-20].

The specific causes of prostate cancer are unknown. [21] The risk of developing prostate cancer is associated with genetics [22], the race [23], the diet [24], lifestyle and medication. [25] However, the primary factor for this disease is known as the age. Prostate cancer is rare in men below the age of 45, and becomes proportionally increased with the age. The average age at diagnosis is 70 years [26].

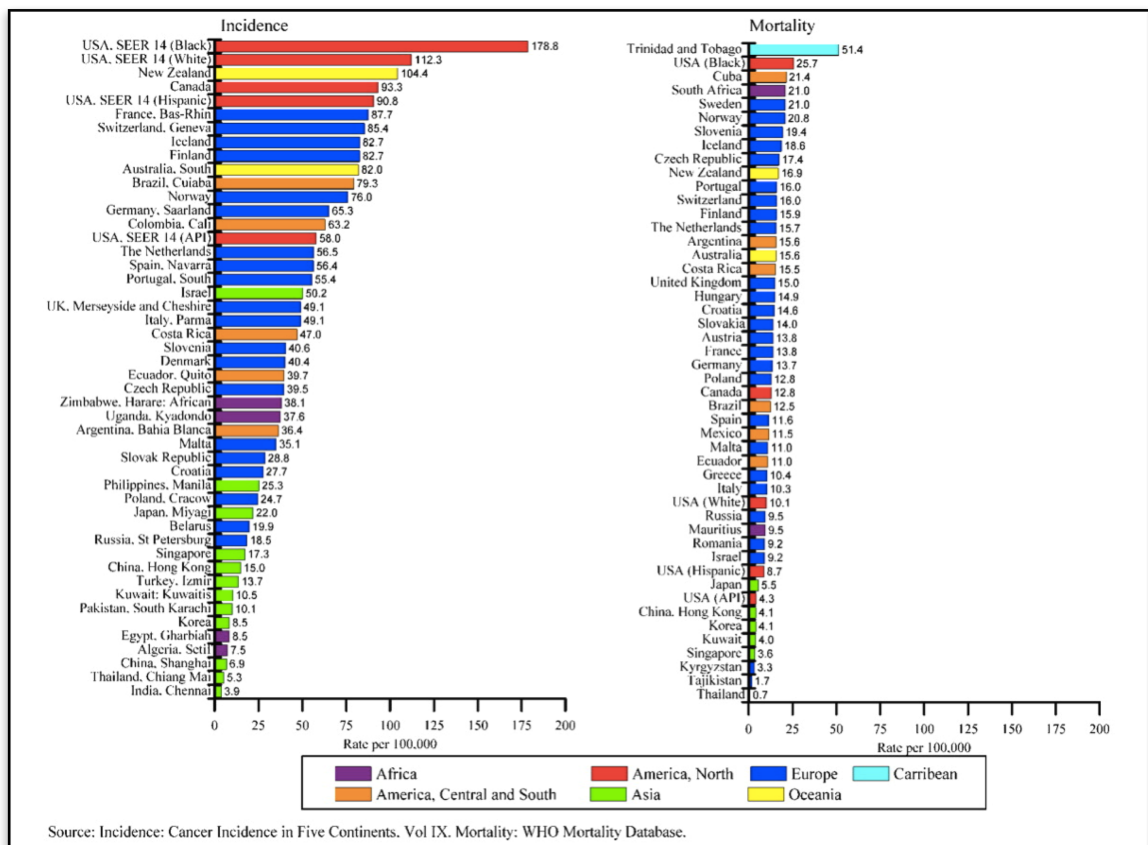


Figure 1.2. The Prostate Cancer Incidence and Mortality Rates Between 1998 to 2002 [26]

1.4. PATHOLOGICAL STAGES OF PROSTATE CANCER

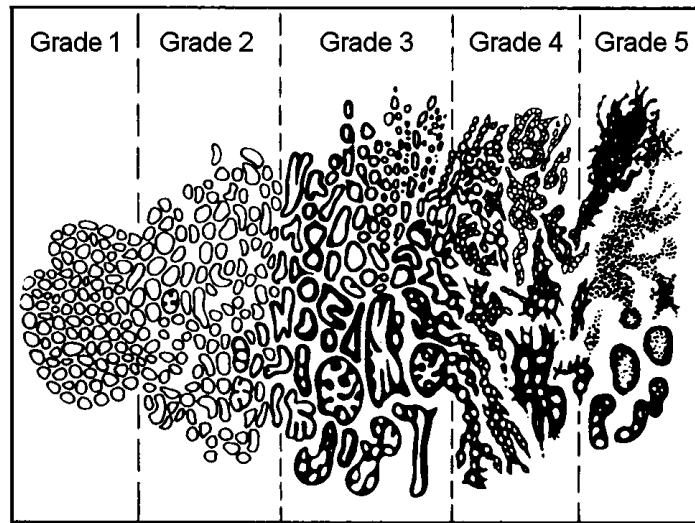
1.4.1. TNM Classification System

TNM classification system is a universal and simple system developed to define the anatomical extent of a cancer. T gives information about the tumor diameter, N states the invasion of the local Lymph Nodes by cancer cells and M tells if there is any metastasis. According to this classification, there are T0, T1, T2, T3, T4, N0, N1, N2, N3n, M0 and M1. If no primary tumor is detected, the specimen is evaluated as T0 stage. If the tumor is less than one cm in diameter the tumor is classified as T1, tumor is in T2 stage if tumor diameter is greater than one cm in diameter. If the vessel is spread independently to adjacent organs or tissues, it is T3 but if spread in distant organs and tissues is detected it is known as T4 stage. No regional lymph node metastasis defined as N0 while N1 means there is metastasis to the lymph nodes on the same side of the tumor, N2 represents to the metastasis to distant lymph nodes on the same side and finally N3 represents the metastasis to the contralateral lymph nodes. [13]

1.4.2. Gleason Score

The Gleason system is used for the evaluation of the prognosis in prostate cancer. In this system, prostate biopsy samples are investigated. As a result of the histological examination of cancerous tissue, benign glands, paraneoplastic foci (PIN) and different grades of neoplastic foci can be seen in the same area. Regarding this heterogeneity, Gleason developed a grading system that is now considered a good prognostic indicator. (Gleason, 1992).

The Gleason score range is between 2 and 10. To determine the degree of tumor, the pathologist scores each piece of tissue taken from the biopsy and specifies the sum of the two most common values to determine the Gleason sum score. Scores between two and four are defined as low aggressiveness (spreading awareness). Gleason 6 and 7 score showed higher aggressiveness, whereas Gleason 8, 9, and 10 score tumors were found to be scattered in the area where the tumor is usually located.



1.3. Histological Grades of Prostate Cancer According to the Gleason Grading System.

[13]

Small and well differentiated tumors (grade 1 and grade 2) are usually organ-confined, large (greater than 4 cm³) and poorly differentiated tumors (4th and 5th grade) are usually local advanced or metastatic. Gleason score 2-4 represents well differentiated tumor while Gleason score 5-7 represents moderate differentiated tumors and Gleason scores 8-10 represent poorly differentiated tumors. [13]

1.5. MOLECULAR MECHANISMS IN THE DEVELOPMENT OF PROSTATE CANCER

Mechanisms responsible for the formation and the progression of prostate cancer have not been completely discovered yet. However, changes in many different signal transduction pathways controlling cell growth, cell proliferation, angiogenesis and cell adhesion is considered to have a role in the development of prostate cancer. The progression of the prostate epithelial cells from the normal state to the malignant state is accompanied by a combination of proto-oncogene activation and tumor suppressor gene suppression.

The molecular signaling pathways that play an important role in the development prostate cancer are PTEN, the phosphatidylinositol-3-OH kinase (PI3K) pathway and the downstream pathways of the androgen receptor (AR), vascular endothelial growth factor

receptor (VEGFR), and Insulin growth factor 1 receptor (IGF1R). In particular, PI3K / Akt pathway plays an important role in the development and progression of prostate cancer. This pathway is often activated by the reduction of tumor suppressor protein, PTEN expression, in prostate cancer cells. [32-33-34]

1.5.1. PI3 kinase / Akt signaling pathway and PTEN in Prostate Cancer

Phosphatidylinositol-3 kinase (PI3K) is a protein responsible for the transmission of growth and survival signals. Receptor tyrosine kinase (RTK) in response to mitogenic ligands, activates PI3K. The PI3Ks phosphorylate PIP2 (phosphatidylinositol (4,5) bisphosphate) to PIP3 (phosphatidylinositol 3, 4, 5 triphosphate). The resulting PIP3s, on the other hand, affect protein GTPase regulators and skeletal proteins. [58]

The extracellular signal enables the RTK (receptor tyrosine kinase) to be active. Inactive PI3K is activated by binding to the phosphorylated tyrosine of RTK with SH2 domains. The active PI3K catalytic units convert PIP2 to PIP3. In the cytosolic part of the cell membrane, with the increase of PIP3, Akt and PDK1 proteins are linked to PIP3 by their PH domains found in their structures. Thus, Akt and PDK1 are retained on the cell membrane. PDK1 phosphorylates and activates Akt. [58]

Cytokines and growth factors act on the Akt and PI3K pathways to generate survival signals for the cells. The stimulation of Protein kinase B affects the activities of various proteins in the cell. One of these is the mammalian target of rapamycin (mTOR) protein [50]. The significant losses of PTEN function in the formation of tumors; Akt, which is the best known effector of PI3K in this pathway, can be easily phosphorylated.

To sum up, PI3K, stimulated by growth factors, phosphorylates PIP2, bound to cell membrane, and converts it to PIP3. PIP3 is a secondary message molecule that activates an oncoprotein, the Akt molecule. Active Akt molecule phosphorylates cytoplasmic kinases, transcription factor and the cell cycle regulator molecule, and caused the transmission of stimulatory signals to the nucleus. PTEN deactivates lipid mediator PIP3 by dephosphorylating it with lipid phosphatase function. The tumor suppressor property of PTEN is derived from this lipid phosphatase function. Increased intracellular PTEN and consequent Akt inactivation, is caused to G1 arrest and apoptosis in the cell cycle. Cell proliferation is increased in cells without PTEN function.

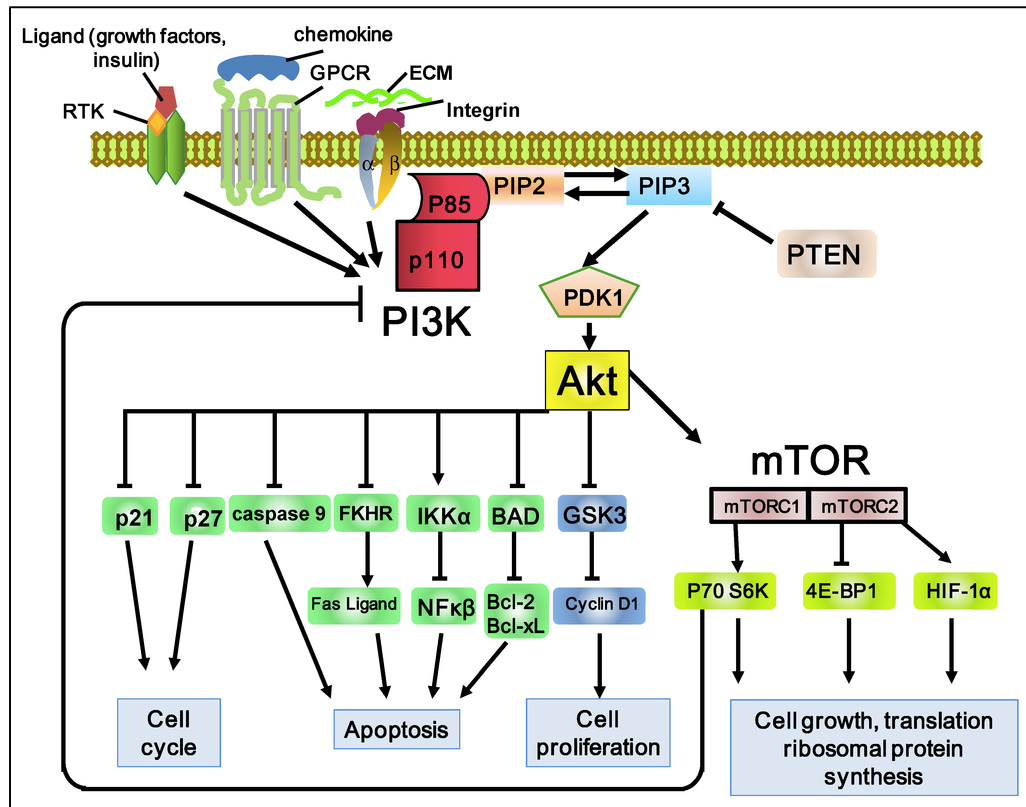


Figure 1.4. PI3K/Akt/mTOR Pathway [56]

The PTEN gene is a tumor suppressor gene located outside the cell nucleus, which is a 47-kDa, tyrosine phosphatase and tensin homologue, containing 403 amino acids, located on the 10q23.3 chromosomal regions. The name of PTEN comes from the protein tyrosine phosphatase and tensin homology. PTEN was found incidentally while researching for the tyrosine phosphatases. PTEN is a dual phosphatase with both protein and lipid phosphatase activity and it is the first known tumor suppressor molecule to have an enzymatic function [42]. The first reason for PTEN to be considered as a tumor suppressor gene is that it dephosphorylates phosphoproteins and PIP3. Hence PTEN antagonizes the PI3K activity and controls cellular functions such as cell growth, proliferation, and cell cycle. [44]

PTEN functions in the PI3K/Akt pathway, which transduces signals into the cell from the extracellular molecules such as growth factors and cytokines that stimulate cell growth and proliferation by receptor tyrosine kinases.

PTEN plays a negative regulatory role on PI3K / Akt pathway. PI3K / Akt pathway regulates important cellular events in prostate carcinogenesis. Activation of this pathway in prostate cancer has been shown to be associated with more advanced stage, worse prognosis, and higher Gleason score. [13] In addition, it has also been determined that phosphorylated Akt is highly detected in prostate cancer tissue observed by immunoblotting, which can predict biochemical recurrence. This pathway can also be activated by VEGFR and IGFR-1. There is also interaction between AR (Androgen Receptor) and this pathway. [54]

In later stage prostate cancers and metastatic tumors, PTEN frequently lost its genetic function. [56] Homozygous PTEN deletions occur in the early stages of patients and are highly likely to have metastasis. Prostate cancer develops rapidly as a consequence of a decrease in PTEN expression due to genomic instability of a close range of genes, resulting in PI3K / Akt pathway activation and uncontrolled cell proliferation. [56]

1.6. ANDROGEN RECEPTORS IN PROSTATE CANCER

The development, differentiation and maintenance of prostate gland is regulated by the hormones called androgens. Androgens are sex steroids hormones, including testosterone, dihydrotestosterone (DHT). 90 per cent to 95per cent of these androgens are produced from testes, and about 5 per cent are from adrenal. 95 per cent of testosterone entering the prostate cell is transformed into DHT via 5 α -reductase. Although testosterone is the main circulating androgen in the body, the affinity to the androgen receptor (AR) of DHT is 10 times more potent and DHT is more stable ligand for AR. [31]

AR, or NR3C4 (nuclear receptor subfamily 3, group C, member 4), are steroidal nucleus receptors, which are found in the cytoplasm of prostatic epithelial and stromal cells bound to the Heat-Shock Protein (HSP) under the physiological conditions. DHT binding to the androgen receptor leads to its separation from HSPs, which is then phosphorylated. [97] The phosphorylated AR then undergoes conformational changes resulting in the nuclear translocation of the DHT-AR complex where it binds to the Androgen-Response Elements (ARE) in the promoter region of the target genes. Co-activators and co-repressors also bind to the AR complex to facilitate or prevent the transcription of the AR-target gene.

Activation of target genes results in biological responses involving growth, survival and PSA production events. In vitro studies have shown that certain coactivators such as ARA54, ARA55, ARA70, ARA160, p160, BRCA1, AIB1 and CBP (cortisol binding protein) either increase or decrease the transcriptional activity of AR. In the nucleus, prostate cell metabolism is regulated by the transcription of androgen-responsive genes, in that activation or suppression of target genes regulates prostatic cell growth, proliferation, PSA production and life span. [98]

In addition, it has been reported that AR has developed different evolutionary aberrations as a result of sequential treatments. There are publications reporting that changes such as increased number of androgen gene copies, AR variants allowing ligand-independent activation, mRNA overexpression, mutations in the AR-ligand binding domain could be the cause of hormone refractoriness and antiandrogen resistance. [99]

Expression of the androgen receptor is preserved during prostate cancer and most androgen-independent or hormone-resistant prostate cancers represent the androgen receptor. As shown in figure 1.5. Hormone-dependent androgen receptor signaling is mediated by dihydrotestosterone stimulation of the androgen receptor. (left panel) Hormone-resistant prostate cancer cells survive by stimulation of multiple signaling pathways, including PI3K and MAPK pathways. These are known as alternative pathways leading to androgen receptor signaling or cell proliferation, migration and also cell survival. (Right panel) [33]

The mutation of AR may have a role in the progression of prostate cancer and the failure of endocrine therapy which is caused by the AR transcriptional activation by activating anti-androgens or other endogenous hormones. In addition to this, changes in the expression of AR co-regulators may have a role in the prostate cancer progression and could be the cause of AR ligand specificity or transcriptional activity. [32 33 34]

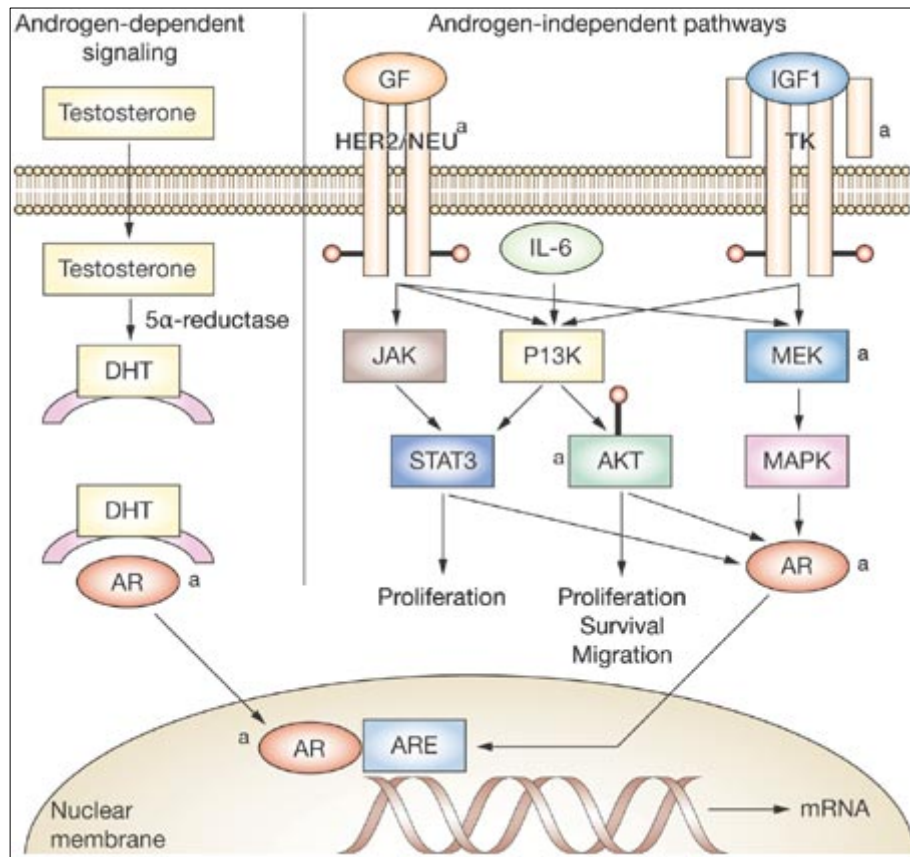


Figure 1.5. The Mechanism of the Androgen Receptor [33]

1.7 PROGNOSTIC SIGNIFICANCE OF INSULIN-LIKE GROWTH FACTOR-1 RECEPTOR (IGFIR) EXPRESSION IN PROSTATE CANCER

In recent years, the physiology of the prostate tissue has been better understood that's why genetic and molecular mechanisms, growth factors and receptors have been prognostically evaluated for the prostate cancer development [64]

Insulin-like growth factor (IGF) is a polypeptide which is structurally similar with proinsulin, IGF has both mitogenic and metabolic activities due to the binding of IGF-1 to the cell surface receptors. Insulin and insulin-like growth factor-1 (IGF-1) signal negatively regulates the fork head box protein family, FoxO, especially Foxo-1 and relevant biological functions controlled by this transcription factor. IGF-1 may also potentiate the androgen signaling through AR activation. As Foxo-1 is a novel nuclear repressor for AR, IGF-1 / insulin signaling can provide stimulatory effects on AR by weakening Foxo-1 action. The phosphorylation and inactivation of Foxo-1 by IGF-1 or insulin-induced phosphatidylinositol-3-kinase (PI3K) / Akt kinase and abolishes its

inhibitory effect on the AR transactivation. [64-65] According to the literature, IGFR has been shown to play an important role in the development and progression of brain, breast, thyroid, kidney, colon, stomach, liver tumors and malignant melanoma. [66] IGFR has also been shown to be effective in the development of resistance in cancer treatment. Studies also show that IGFR activation plays an active role in benign hyperplasia, dysplasia, and carcinogenesis, by giving proliferative signals in the prostate tissue. In addition, the activation of IGFR pathway increases cell migration capacity in androgen-independent prostate cancer cells and leads to a drug-resistant phenotype. [66]

These findings have shown that IGFIR plays an important role in prostate cancer biology, and IGFIR-targeted therapies may also be considered as an alternative treatment approach in both treatment-resistant and metastatic prostate cancer. [65]

1.8 VASCULAR ENDOTHELIAL GROWTH FACTOR IN PROSTATIC CANCER

Vascular Endothelial Growth Factor, VEGF is the most specific mitogen as known for endothelial cells which plays an important role in vasculogenesis and angiogenesis. According to the literature, the binding of VEGF to vascular endothelial growth factor receptor, VEGFR, activates the intracellular signal transduction pathways including PI3K/Akt/mTOR and MAPK pathways in the vascular endothelial cell, thereby increasing the uncontrolled survival of the endothelial cell and also the neovascularization. Addition to these studies, increased in VEGF expression has a critical effect on the growth and progression of prostate cancer. [67] VEGF plasma levels have been shown to be an independent prognostic factor in the metastatic prostate cancer such that prognosis is worse in patients with high VEGF plasma levels. [67]

So far is known, androgen ablation is one of the primary therapies used to prevent metastasis in prostate cancer. Since prostate cancer cells are initially androgen dependent, the suppression of testosterone and dihydrotestosterone levels reduces the rate of growth in prostate cancer cells. However, in the continuation of this initial response, prostate cancer cells may become resistant to castration and may also develop a more aggressive phenotype with their proliferative potential and increased VEGF expression. Since VEGF

has been implicated in tumor angiogenesis and cell proliferation, it has come to the fore that therapies targeting VEGF pathways are promising and clinical investigations VEGF targeting have been accelerated. [67]

1.9. CELL DEATH MECHANISMS

Regardless of the oncogenic pathway that is activated in the prostate cancer, evasion of the programmed cell death is at the top of cancer cell survival mechanisms. [30]

The apoptosis signaling platform is divided into two central apoptotic pathways known as intrinsic and extrinsic pathways as sources of cell death inducing phenomena.

The extrinsic pathway which is known as death receptor dependent pathway is triggered by the binding of the Tumor Necrosis Factor (TNF), the FAS ligand or the TNF-related apoptosis-inducing ligand (TRAIL) to the relevant death receptors. Once activated death receptors recruits the death receptor adaptor proteins which in turn leads to the recruitment and activation of the initiator caspase pro-caspase 8 protease. The active caspase 8 then activates caspase cascade, which cleaves the cytoskeletal proteins and nucleus skeleton and activates DNase enzymes which causes the breakdown of cell DNA. [30]

To mention in detail, apoptotic signaling mediated extrinsic pathway starts with the binding of extracellular ligands such as TNF, Fas-L and TRAIL to the extracellular ligand binding domain of transmembrane receptors. Following ligand-receptor binding, death receptors expose their intracellular dead domains which associates with a correlative protein motif in adapter proteins called Fas-associated death domain (FADD) and the TNF receptor-associated death domain (TRADD) adapter proteins. The FADD and TRADD adapter proteins possess another domain of protein interaction called the Death Effector Domain (DED) which interacts with DED of pro-caspase-8 forming leading to the formation of death-induced signal complex (DISC) and activation of this initiator caspase. [30-31]

The intrinsic apoptotic pathway initiates with the intracellular signals which accrete in mitochondrial level due to the stress conditions such as DNA damage, oxidative stress, and oncogene activation. Following the internal stimuli, pro-apoptotic bcl-2 proteins actively facilitate the formation of Bax-Bak channels in the outer mitochondrial membrane which causes the release of cytochrome-c protein. Cytochrome-C interacts with apoptosis stimulating factor (AIF) in the cytoplasm leading to the formation of apoptosome complex. [31] The apoptosome complex causes to the activation of initiator caspase, caspase 9 which activates executioner caspase 3, 6 and 7 and initiates caspase cascade resulting in cell death.

When endogenous apoptotic signal initiates, BIK (Threonine (33) and Serine (35) protein is phosphatized by casein-like kinase-II and transfer from the endoplasmic reticulum to the mitochondria and BIK protein attached to the anti-apoptotic Bcl-2 and Bcl-xL proteins. Bcl-2 and Bcl-xL proteins bind to Bax and Bak proteins in healthy cells, to prevent these proteins from forming pores on the mitochondria. The binding of the Bik protein to the Bcl-2 and Bcl-xL proteins frees Bax and Bak proteins to form homo- or hetero-oligomer complexes of the channel triggering apoptosis. [27-30]

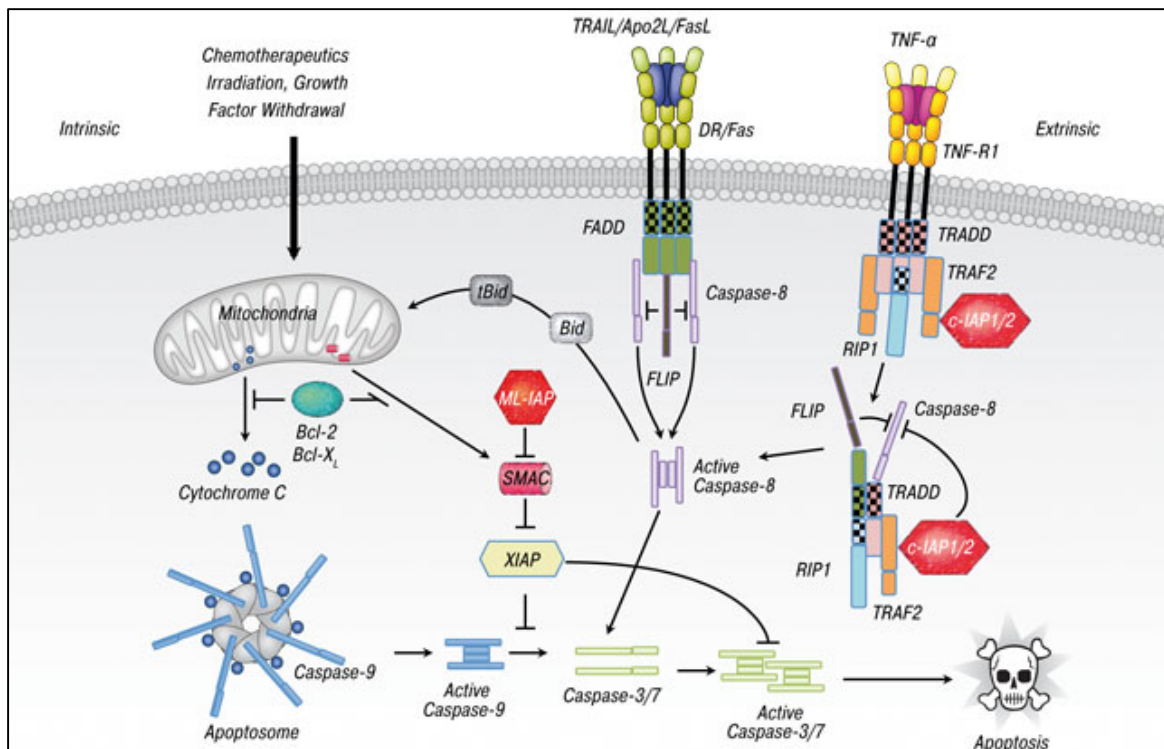


Figure 1.6. The Intrinsic and Extrinsic pathway of Apoptosis [57]

The Bcl-2 family consists of the apoptosis regulator Bcl-2 and its homologs. These proteins direct mitochondrial outer membrane permeabilization (MOMP) and may be pro-apoptotic such as Bax and Bak or anti-apoptotic including Bcl-2 and Bcl-x_L. There are a total of 25 genes known to date in the Bcl-2 family. [69] The members of the Bcl-2 family participated in one or more of the four characteristic domains of homology entitled the Bcl-2 homology domains which is named as BH1, BH2, BH3 and BH4. The BH3-subset of the Bcl-2 protein family has only one BH3-domain. BH3-only family members are known to play an important role in promoting apoptosis known as Bim, Bid and Bik. BIK is the constitutive member of the BH3-only family of apoptotic proteins. [69] BIK is predominantly localized in the endoplasmic reticulum and induces apoptosis along the mitochondrial pathway by activating calcium from the ER to the mitochondria and remodelling the mitochondrial cristae. BIK-mediated apoptosis mediates selective activation of BAX. BIK protein consists of 160 amino acids and contains a transmembrane domain addition to the BH3 domain. It has been shown that BIK, Bcl-2 interacting killer, is phosphorylated on Thr (33) and Ser (35) by a casein kinase II-like kinase, and mutations that inhibit phosphorylation reduce cell death activity and interaction with anti-apoptotic

proteins. Mutations mimicking phosphorylation (Thr, Ser to Asp) increased cell death activity of BIK and also increased the interaction with BCL-xl and BCL-2. [70]

It has been shown for the first time that BIKDD (T33D, S35D), a mutant of Bik which was identified by the Liu et al, mimics the phosphatidyl form of the BIK protein and binds to Bcl-2 and Bcl-xL proteins and thus activates apoptosis pathway. In the follow-up studies, It is shown that BIKDD has also causes cancer cell destruction such as pancreatic, lung and breast. [69-70]

Another gene that is widely used for apoptosis-inducing, anti-cancer is the BIKDDA gene. [38] BIKDDA has a longer life span and higher apoptosis-inducing effect than BIKDD gene. [60] That's why it has been used as an attractive therapeutic agent for the treatment of various cancers. In recent years' studies have shown that the BIKDDA triggers the death of various prostate cancer cells. [58-60]

1.10. THERAPY STRATEGIES OF PROSTATE CANCER

Today, there are many methods developed for the treatment of prostate cancer. Combining treatment methods ensures successful results when radiotherapy, chemotherapy or surgery alone is mostly unsuccessful. If the cancer is located within the prostate tissue it is possible to remove it by operation. [14] After removal of tumor tissue, additional treatment is required using radiotherapy or chemotherapy. However, chemotherapy is not effective in hormone-independent prostate cancer and is used only as relaxation therapy. [15] Chemotherapy can be performed after treatment for reducing hormone levels. To reduce hormone levels, hormone agonists or antagonists could also be used. Prostate cancer is a type of cancer composed of heterogeneous cells and chemotherapy alone does not work enough because each cell responds differently to the cancer drugs. [15]

According to the study conducted by Dahhlof et al, the chemotherapeutic drugs that are found to be effective in prostate cancer among many developed cancer drugs belong to the taxane group drugs. Docetaxel and paclitaxel are the most well-known cancer drugs from the taxane group. These drugs work by halting cell division by stabilizing microtubules, which are cell skeletal molecules. These two drugs, which bind to proteins associated with

microtubules and inhibit microtubules, can be used in combination with some other chemotherapeutic drugs such as the alkylating antineoplastic agent estramustine. Docetaxel is the most effective chemotherapeutic drug against prostate cancer and is used in combination with estramustine. [16] The general mechanism of Docetaxel is the inhibition of microtubule depolymerization. Tubulin binds to β subunits and maintains the microtubules at the polymerized level. Docetaxel also leads to the phosphorylation of anti-apoptotic proteins (bcl-2), thereby eliminating apoptotic protection mechanisms and accelerating cell death. [17]

1.11. TARGETED THERAPIES IN PROSTATE CANCER

Today, the most studied and promising approach to cancer treatment is to transport the active ingredients with nanoparticle drug delivery systems. Various nano-carriers, including polymersomes and liposomes, have been used for this purpose. [75] While nano-carriers have many advantages as drug delivery systems, they are rapidly caught by plasma proteins called opsonins in the reticuloendothelial system (RES) organs, primarily in the liver (within about 30 minutes) when administered systemically. RES is comprising a network of cells such as bone marrow, blood, lymph nodes and connective tissue, and organs such as spleen, liver, lungs. Entrapment of nanoparticles within RES and nonspecific organ uptake leads to the shortening of nano-carrier circulation half-life which in turn limit their ability as drug delivery systems. [75]

One of the most important approaches to extend circulation survival times of nano-carriers is to coat the surface of the nano-carriers with a hydrophilic polymer. Natural or synthetically derived hydrophilic polymers such as polyethylene glycol (PEG), chitosan and polyvinyl alcohol (PVA) have been used to modify the surface of the nano-carriers to improve circulation times. [76] PEG is the most commonly used hydrophilic polymer for this purpose, albeit to its disadvantages about oxidation. The poly (2-ethyl-2-oxazoline) (PEtOx) units are thought of as possible candidates with the desired properties to eliminate the solubility problems with PEG [76]. Hence PEtOx units creates a new polymeric platform for biomedical applications with high biocompatibility, stealth effect, low average molecular distribution, responsiveness, high functionalization properties and versatility in the copolymerization properties. [76] The use of PEtOx as an indirect food supplement has

been approved by the FDA and also approved for the medical use, due to this situations, it is expected that the use of biomaterials based on PEtOx will grow very rapidly. [77] It is known that poly-oxazoline polymers exhibit cellular suitability *in vitro* due to exhibiting similar invisibility behavior to PEG and due to their peptide mimicking properties. [78] Most of the polymers in the PEtOx structure studied for *in vitro* cytotoxicity are usually found to be non-toxic. [78]

Polymersomes have applications in the literature, such as nano reactors, imaging agents, drug transportation and active targeting. The greatest reason for its use in drug delivery is that it has a double layered amphiphilic membrane structure similar to the cell membrane, the ability to carry various chemical agents, the ease of application of chemical modifications, a higher stability and loading capacity in comparison with other effective carrier systems, and finally it has no aggregation and toxicity. [79]

Studies aimed at development of targeting chemotherapy drugs to cancer cells have a crucial role in the development of existing targeted therapies for cancer. In recent years, peptides have attracted attention as targeting agents for the delivery of cytotoxic drugs to the tumor location. To date, specific markers were identified for prostate cancer including prostate-specific antigen (PSA), prostate stem cell antigen (PSCA), prostatic acid phosphatase (PAP) and prostate-specific membrane antigen (PSMA). In recent years studies have shown that monoclonal antibodies labeled with radioactivity developed against the PSMA receptor provide successful results in the imaging of prostate cancer (26), compared to other prostate cancer-specific agents. [80]

The prostate-specific-membrane antigen (PSMA), which was first discovered in 1997 by Kawakami et al. is overexpressed in the prostate cancer. In the early detection of prostate cancer, prostate specific antigen (PSA) imaging has reduced mortality. However, the measurement of PSA level on its own, is not sufficient enough to distinguish cancer patients with negative biopsies. [81] In contrast, prostate cancer patients have a high frequency of prostate-specific membrane antigen (PSMA) overexpression at all stages and grades. For this reason, PSMA is an alternative to PSA as a diagnostic biomarker. Shen *et al.* have developed high affinity peptide sequences for PSMA and have indicated that these peptides nanoparticles are suitable for conjugation to develop PSMA targeting nanoparticles. [84] According to the recent study, small peptides selectively binding to

PSMA positive cells may be used for selective delivery to malignant sites as an alternative to antibody-based anti-PSMA therapies. [85] According to the literature, fluorescently labeled dimeric peptides did not show significant binding to PSMA-negative cells such as PC-3 and DU-145, while these peptides specifically bind to PSMA-positive prostate cancer cells such as LNCaP, CWR22R *in vitro* conditions. Additionally, DiPaola et al. investigated the efficacy, safety and pharmacokinetics of peptide-doxorubicin conjugate targeting PSMA in prostate cancer patients. The specific binding of peptide-PSMA targeting prostate cancer cells could be used as targeting agent. [83-84-85]

1.12. AIM OF THE STUDY

Since targeted gene therapy is the latest approach in the treatment of cancer, the aim of this study is to develop a new approach to specifically target prostate cancer using new generation nano carriers carrying a pro-apoptotic gene which has not been used in the treatment of prostate cancer before. For this purpose, a Poly(2-ethyl-2-oxazoline) (PEtOx) based multifunctional carrier systems was used to prepare polymersome nanoparticles carrying the pro-apoptotic gen BIKDDA. To specifically target the prostate cancer, a comparative study was aimed to be performed between healthy and prostate cancer cell lines using three different peptides designed to recognize the PMSA antigen.

2. MATERIALS

2.1. INSTRUMENTS

The instruments which were used during the study was listed below:

- Laminar flow cabinet (ESCO Labculture Class II Biohazard Safety Cabinet 2A, Singapore)
- CO₂ incubator (Nuair NU5510/E/G, USA)
- Fluorescence Microscope (Nikon 80i Eclipse Fluorescence Microscope)
- Centrifuge (Hettich mikro 22R and SIGMA 2-5 centrifuge, Germany)
- Vortex (Stuart SA8, UK)
- pH meter (Hanna instruments PH211, Germany)
- Mini-PROTEAN Tetra Cell Electrophoresis System (Bio-Rad 165-8001, USA)
- ChemiDOC XRS+Gel Imaging System (Biorad Universal Hood 2 (USA)
- Mini Trans-Blot Cell Blotting System (Bio-Rad 170-3935, USA)
- Heater (Bioer,MB102, China)
- 80 °C freezer (Thermo Forma -86 C ULT Freezer, USA)
- ELISA plate reader (Bio-Tek EL x 800, USA)
- Magnetic Stirrer (Heidolph MR 3004, Germany)
- FACS Calibur (BD Biosciences, USA)

2.2. EQUIPMENTS

The laboratory equipments are:

- Serological pipets 25,10,5, two ml (Grenier Bio or Axygen, USA)
- Micropipettes 10 μ L, 20 μ L, 100 μ L, 200 μ L, 1000 μ L (Eppendorf Research, Germany)

- Polypropylene centrifuge tubes, 50 ml, 15 ml, two ml, one ml, 0.5 ml (Isolab, Germany)
- Cell culture flasks, T-25, T-75, T-150, multiple-well cell culture plates, and cryovials (TPP Switzerland or Grenier-Bio, Germany)
- Electronic pipette (CAPP aid, Denmark)
- Pipette tips 10 μ L, 100 μ L, 200, 1000 μ L (CAPP Expell Plus, Denmark)
- Filter 0.22 μ m (TPP, Switzerland), 0.45 μ m (Santorium Stedim_Biotech, Germany)
- Bright-Line™ Hemacytometer (Sigma Aldrich, Z359629, USA)
- Cover Slip (Sigma Aldrich, [Z375357](#), USA)
- Graduated Cylinder 50 mL, 250 mL, 500 mL, 1000 mL (Isolab, Germany)
- Whatman paper (Isolab, Germany)

2.3. CHEMICALS

2.3.1. Cell Culture Media:

- Dulbecco's Modified Eagle's Medium, high glucose (Gibco 41966),
- RPMI 1640, Sigma, R8758,
- EMEM, Lonza, 12702, DMEM F12,
- Lonza, BE-12-719F,
- Opti-mem, Gibco 31985-070

2.3.2. Growth Supplements:

- Fetal Bovine Serum (FBS) cell culture tested (Sigma F9665, Germany)

2.3.3. Other Reagents:

- 2-propanol (AppliChem A3928, Germany)
- Absolute Ethanol (AppliChem A3678, Germany)
- Acrylamide/ Bis-acrylamide (29:1) (Sigma A3574)
- Ammonium Persulfate (APS) (BioRad, 1610700, USA)
- Bovine Serum Albumin (Santa Cruz, sc-2323, USA)
- Collagen Type-I from Human Placenta (Sigma C7774)
- Dimethyl sulfoxide (Santa Cruz sc-202581, USA)
- Dulbecco's Phosphate Buffered Saline (DPBS) (PAN Biotech P04-53500, Germany)
- Ethylenediaminetetraacetic acid (EDTA) (Merck, K40173218 946, Germany)
- Glycine (Merck 104169)
- 4-(2-hydroxyethyl)-1-piperazineethanesulfonic acid (HEPES) (Multicell 600-032-EG, Canada)
- Phenylmethanesulfonylfluoride (PMSF) (Sigma 78830, USA)
- Protease Inhibitor (PI) (Sigma, P8340, USA)
- Penicillin-streptomycin (Thermo Scientific SV30010 or Biochrom A2213, Germany)
- Protein Assay Reagent A (BioRad, 5000113)
- Protein Assay Reagent B (BioRad, 5000114)
- Polybrene (Santa Cruz, sc-134220)
- Sodium orthovanadate (Na_3VO_4) (Sigma, S6508, USA)
- N,N,N',N'-Tetramethylethylenediamine (TEMED) (Sigma, T7024, USA)
- Trypsin-EDTA (Biochrom L2153, Germany)
- Tris-base (Merck 108387)
- Tris-HCl (Merck 108219)
- Triton-100X (Biomatik Corporation, A4025)
- Trizol (Invitrogen, 15596-018)
- Trypan Blue dye (Sigma, 076K2331)

- Tween-20 (Merck, 822184)
- LB Broth (Sigma, L3522)
- LB Agar (Fluka, B6768)
- Xtreme Gene HP DNA transcription reagent, (Roche, 20382)

2.4. KITS and SOLUTIONS

- Amersham Hybond- ECL Nitrocellulose Membrane (GE Healthcare RPN303D)
- Amersham Rainbow Protein Marker (GE Healthcare RPN800E)
- Bovine Serum Albumin, Protein Standard (Sigma P0834)
- Clarity™ Western ECL Substrate, (BioRad, 1705061,USA)
- RIPA Lysis Buffer (Santa Cruz sc-24948, USA)
- PVDF membrane 0.45 µm, 26.5 cm x 3.75 m (ThermoFisher Scientific, 88518 , USA)
- QuantiTect SYBR Green PCR Kit (Qiagen, 204145, USA)
- Sensiscript RT Kit (Qiagen, 205213, USA)
- Quick Change Lightning Site-directed Mutagenesis Kit (Agilent technologies)
- XL-Gold Ultra Competent Kit (Agilent technologies)
- Ultrapure Plasmid Isolation Kit (Invitrogen)

2.5. ANTIBODIES

2.5.1. Primary Antibodies

- Rabbit- anti-Bik Antibody (Cell Signaling-4592S, USA)
- Mouse-anti-TRAIL Antibody (Abcam, AB42121)

2.5.2. Secondary Antibodies

- Anti- rabbit IgG Peroxidase Conjugate (Sigma A0545)
- Anti- mouse IgG Peroxidase Conjugate (Sigma A4416)

2.6. CELL LINES

- 22RV1, Homo sapiens, prostate carcinoma Adherent (ATCC Number: CRL-2505)
- PNT1A, Homo sapiens, prostate normal Adherent (ATCC Number: CRL-11609)
- HDF, Primary human fibroblast, Adherent (ATCC Number: PCS 201-012)
- HEPG2, Liver healthy, Adherent, (ATCC Number: HB-8065)
- HFOB1.19, Homo sapiens, bone Adherent (ATCC Number: CRL-11372)
- HUVEC, Primary Umbilical Vein Endothelial Cells, Adherent (ATCC Number: CRL-1730)

3. METHODS

3.1 CELL CULTURE METHODS

3.1.1. Cell Types and Culturing Conditions

The prostate epithelial cell line PNT1A was obtained from Sigma Aldrich and two prostate cancer line lines 22RV1 (androgen independent), LnCap (androgen dependent) were obtained from ATCC (American Type Cell collection). These cell lines were cultured in RPMI-1640 media, both supplemented with 10% (v/v) FBS (Fetal Bovine Serum) and 100 units/ml Penicillin and 100 μ g/ml Streptomycin (1% PS). In addition, primary human dermal fibroblast (HDF), human fetal osteoblastic 1.19 cell line, hFOB 1.19(CRL-11372), liver hepatocellular carcinoma, HEPG2 (HB-8065) and human umbilical vascular endothelium cell line, HUVEC (CRL-1730) cells were obtained from ATCC. HDF cells were cultured in Dulbecco's Modified Eagle Medium (DMEM) completed with 10% FBS and 1% PS. Hfob1.19 cells were maintained in DMEM F-12 media and HEPG2 cells were cultured in Eagle's minimal essential medium (EMEM) media, both supplemented with 10% FBS and 1% PS. For HUVEC cell line, F-12K Medium will be used for cultivation with 0.1 mg/ml heparin and 0.03-0.05 mg/ml ECGS supplements.

All cell lines were cultured at 37°C, 5% (v/v) CO₂ and 95% (v/v) air.

3.1.2. Cell Passaging

Cell passaging was performed when cells reached to 70% confluency. The cell monolayer was washed with 1X DPBS pH 7.4 (Dulbecco's Phosphate-Buffered Saline). Cells were detached with 0.05% (w/v) trypsin at 37°C for 3 minutes. In order to neutralize trypsin activity, 10% (v/v) FBS containing media (at two times volume of trypsin) was added and cells were collected. Cell suspension was centrifuged at 300 \times g for 5 minutes, supernatant was discarded and pellet was resuspended in growth media.

3.1.3. Determination of Cell Number

Following the cell passaging protocol, cell pellets were re-suspended in fresh media as described above (Section 3.1.2.). 10 μ l of cell suspension was loaded into the hemocytometer. The middle square of the hemocytometer was counted under the inverted light microscope using $\times 4$ objective. Total cell number per milliliter was calculated with the formula of:

Cell number/ml= 'counted cell number \times dilution factor, factor/ mm² \times chamber depth'.

3.1.4. Cell Cryopreservation

10% (v/v) Dimethyl sulfoxide (DMSO) and 90% (v/v) FBS was mixed for the preparation of the freezing mix solution. Following the centrifugation described as section 3.1.2., cell pellet was resuspended in 1ml of freezing mix solution and placed into a cryovial. Cryovials were immediately put into -80°C freezer. The day after, vials were transferred into the liquid nitrogen to store cells long period of time.

3.1.5. Cell Thawing

Cryovials containing frozen cells were taken from liquid nitrogen and warmed immediately to 37°C. Into the freezing mix 5 ml of pre-warmed growth medium was added drop by drop in order to prevent the sudden increase in the osmotic pressure. Cell suspension was then centrifuged at 300 \times g for 5 minutes. Supernatant was decanted and the cell pellet was suspended in complete growth media (media that contains 10% FBS and 1% PS) followed by the seeding of the cells into tissue culture flasks. The day after, cell medium was collected and replaced with fresh medium to remove any residual DMSO

3.2. ISOLATION AND CHARACTERIZATION OF pEGFP-BIKDDA PLASMID DNA

pEGFP-BIK plasmid, was purchased from Add gene and grown on Luria Broth (LB) Agar. After the colony formation was detected, colonies were selected and grown on 350ml of LB broth.

3.2.1. Plasmid Construction and Site-Directed Mutagenesis

PEGFP BIKDD plasmid was stored in our lab. Site-directed mutagenesis was performed according to the QuikChange Lightning Multi Site-Directed Mutagenesis Kit; Agilent Technologies protocol. Serine 124 of BIKDD was changed to Alanine acid by using the BikDDA F primer: 5'-AACATAATGAGGTTCTGGAGAGCCCCGAACCCC-3' and BikDDA R primer: 5'-GGGGTTCGGGGCTCTCCAGAACCTCATTATGTT-3' (Fig 1).

Thermal cycling reaction was performed with the primers and the reaction reagents as shown in Table 3.1. below.

Table 3.1. PCR (Polymerase Chain Reaction) Components for site-directed mutagenesis

Reaction Ingredients	Sample (BikDDA)	Control
10× QuikChange Lightning Multi reaction buffer	2.5 µl	2.5 µl
Quick Solution	0.5	-
dNTP mix	1 µl	1 µl
Mutagenic primers	1 µl (100 ng)	1 µl
ds-DNA template	1 µl (100 ng)	1 µl
QuikChange Lightning Multi enzyme blend	1 µl	1 µl
ddH ₂ O (final volume: 25 µl)	18 µl	18.5 µl

The reaction was conducted at 95°C for 2 min as the initial denaturation step and followed by 30 cycles at 95°C for 20 sec, 55°C for 30 sec, 60°C for 30 sec, 65°C for 30 sec and 65°C for 150 sec. Final extension step was performed at 65°C for 5 min.

Table 3.2. PCR Conditions

Segment	Cycle	Temperature	Time
1	1	95	2 minutes
2	30	95	20 seconds
		55 or 60 or 65	30 seconds
		65	30 seconds
3	1	65	5 minutes

After the thermal cycling, 1 microliter of DpnI restriction enzyme was added into each reaction mix and then samples were incubated at 37°C for 5 minutes to digest the methylated DNA. The desired mutation was then transformed into XL-Gold component cells provided along using manufacturers protocol (Agilent Technologies). 2 microliter of Betamercaptoethanol was added into the competent cells which were then incubated on ice for 10 minutes. Into the competent cells, 2 microliter of DpnI treated DNA was added and each tube was incubated on ice for 30 minutes. Samples were then incubated in a 42°C water bath for 30 seconds. After this step, samples were incubated on ice for 2 minutes to complete the heat shock process. 0.5 ml of NZY broth or LB broth were added onto each sample and incubated at 42 °C for 1 hour while shaking at 225 rpm. Meanwhile, LB agar plates were prepared by adding 20mM IPTG and 80 µg/ml X-Gal to perform blue white screening method.

250 microliters of transformants were spread onto plates with appropriate antibiotics and was incubated at 37°C for more than 16 hours. White colonies were selected, then a single colony was transferred in 0.5ml of LB Broth with antibiotics and cultured for 24 hours. Upon OD measurement, plasmid isolation was performed as described Section 3.2.2. The sequences of BikDDA mutant constructs were confirmed by the next gen sequencing.

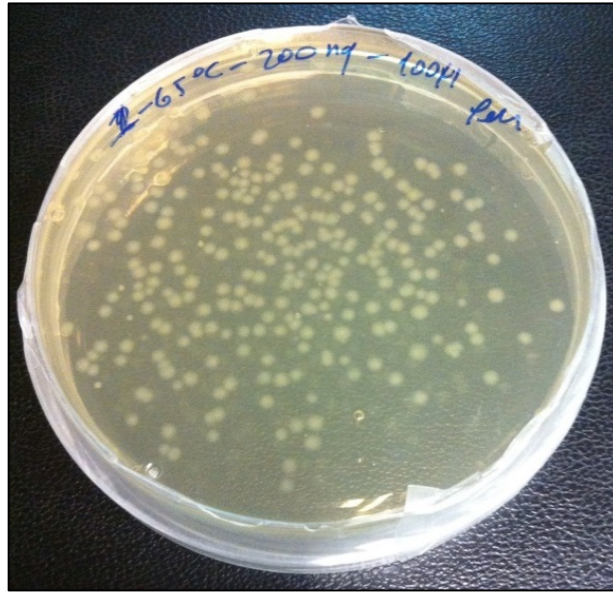


Figure 3.1. Colony formation of BIKDDA transformed with XL-ultra competent cells after 16 hours

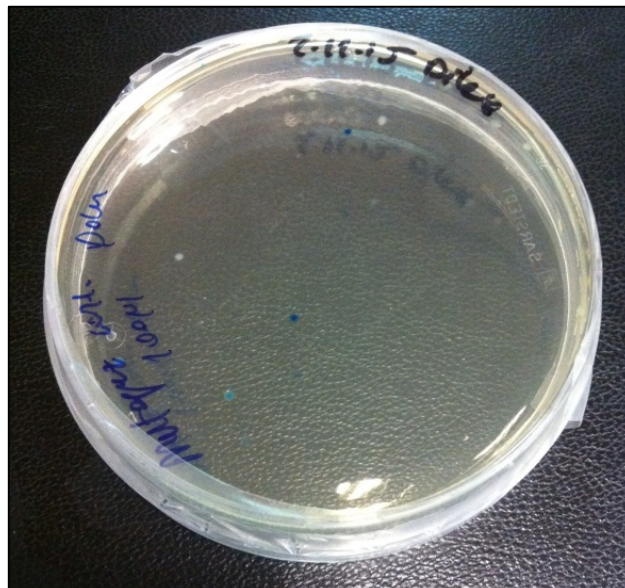


Figure 3.2. Colony formation of control petri plates after 16 hours

3.2.2. Plasmid Isolation

Single colony was picked from the agar plates as previously described in Section 3.2.1 and transferred to the 0.5ml of LB broth. OD value was measured every 2-3 hours at 600 nm.

When the OD Value bacterial culture was between 0.5-0.7, meaning that the bacteria are on the log phase, samples were transferred to the centrifuge tubes and centrifuged at $10.000 \times g$ for 10 minutes and pellet was used for plasmid isolation. Pellet was suspended in 4ml of resuspension buffer with RNase A and gently mixed until it was homogeneous. 0.4ml of lysis buffer was placed onto the cell suspension and incubated for 5 minutes at room temperature. After the lysis step, 4 ml of precipitation buffer was placed into the suspension, which was then centrifuged at $12000 \times g$ for 10 minutes at room temperature. Meanwhile, equilibration column was washed with 10 ml of equilibration buffer. After the centrifugation, supernatant was loaded into the equilibrated column and the solution in the column was allowed to drain by gravity flow. 10 ml of wash buffer was then introduced into the column. In order to collect the purified DNA, first 5 ml of elution buffer was added into the column, then 3.5 ml of isopropanol was placed into the collection tube to elute DNA. Following another centrifugation at $12000 \times g$ for 30 minutes at 4°C. Supernatant was discarded and pellet was washed with 3ml of 70 per cent ethanol. After washing the pellet was dried and suspended in 200 microliter of TE buffer. After the isolation process, the concentration was measured by nano-drop and plasmid DNA was stored at -20°C .

3.3. PLASMID DNA TRANSFECTION

3.3.1. Determination of Transfection Efficiency

22Rv1 cells were seeded into a 24-well plate (2×10^4 cells/well) and incubated for 24h. Transfections were then performed with TRAIL and BIKDDA using Xtreme Gene HP DNA transcription reagent, in Opti-MEM according to the manufacturer's instructions. In order to optimize the transfection efficiency, 1.1, 1.2, 1.3, 1.4, 2.1 ratios of DNA:Transfection reagent were used. Each well was observed and imaged under the fluorescence microscopy at 24h, 48h, and 72h time points. The most efficient concentration and time point was determined and transfection experiments were carried out at these determined conditions.

3.4. DETECTION OF GENE EXPRESSION LEVELS OF TRAIL AND BIKDDA IN 22RV1 CELL LINE

3.4.1. RNA Isolation

300.000 (22RV1) cells were plated into 6-well plate. Following day, plasmid DNA transfection was performed as described section 3.3.1. The day after, starvation was done for 4 hours and then, 6-well plate was taken and placed on ice. Medium was taken. Each well was washed once with 1X PBS pH7.4 (37°C). PeqGold RNA pure solution was added into the each well according to the manufacturers' protocol. Cell suspension in PeqGold RNA pure solution was transferred into 1.5ml eppendorf tubes and chloroform was added onto them. Tubes were inverted several times and then incubated at 25°C for 2-3 minutes. Then samples were centrifuged at 12000 x g for 15 minutes at 4°C. After centrifugation, it was seen that 3 phases were appeared in which the first step was clear phase where the RNA is present. Second phase was yellowish color where proteins were present and in the third phase, DNA was present. So, clear phase was taken and transferred into newly labeled eppendorf tubes. As same as the amount that was taken from the clear phase, pre cooled isopropanol was added and the eppendorf tubes were inverted several times in order to clean the samples. Samples were incubated at 25°C for 10 minutes and then centrifuged at 12000xg for 10 minutes at 4°C. Supernatant was discarded and pre-cooled 75% Ethanol was added onto each sample. Samples were centrifuged at 7500 rpm for 10 minutes at 4°C. Ethanol was discarded and after pellet drying RNase/DNase free water was added into the samples and concentration was measured with nano drop.

3.4.2. Reverse Transcriptase Polymerase Chain Reaction

For the conversion of RNA into cDNA Qiagen Senscript Reverse Transcriptase was used. Master mix was prepared according to the table below. PCR reaction was performed at 37°C for 60 minutes. After reaction, cDNA samples were measured using Nano drop.

Table 3.3. RT-PCR reaction master mix

Reagents	Volume per reaction
10x Buffer	2 μ l
dNTP mix (5mM)	2 μ l
10 μ M Oligo dT primer (from 10X to 1X)	2 μ l
Senscript Reverse transcriptase enzyme	1 μ l
Rnase-Dnase free water	variable
Template	variable
Total reaction volume	20 μ l

3.4.3. Quantitative Polymerase Chain Reaction

The mRNA expression levels of TRAIL and BIKDDA genes were analyzed using Syber-green Quanti-Tech (Qiagen) kit. Reaction mixture was prepared including Syber green PCR mix, universal primer, Rnase-Dnase free water and 500 ng for each sample, and reactions were performed according to the conditions shown in table 3.4.

During the analysis 18S rRNA reference gene was used to make relative quantification and absolute quantification was analyzed using the standard curve.

Table 3.4. Quantitative PCR conditions

Cycle	Temperature	Time	Phase
1	94°C	15 min	
2	95°C	5 min	Initial denaturation
3 (39 repeat)	95°C	60 sec	Denaturation
	55°C	60 sec	Annealing
	72°C	60 sec	Extension
4	72°C	10 min	Final extension
5 (80 repeat)	50-80°C 0.5 °C increase /12 sec		Melt curve
6	4°C	∞	Cooling

3.5. MEASUREMENT OF PROTEIN LEVELS IN 22RV1 CELL LINE

3.5.1. Total Cell Lysate Preparation

22RV1 cells were seeded 300.000cell/well into 6-well plate. Transfection was performed for the cells as described section 3.3. previously. Following day, medium was collected and cell monolayer was washed with PBS the wells is put on the eppendorf and then cells are washed with PBS pH 7.4 and collected to the eppendorf. 60 µl of RIPA (contains 1X TBS, 1% Nonidet P-40, 0.5 % sodium deoxycholate, 0.1 % SDS, 0.004 % sodium azide) lysis buffer containing 1% protease inhibitor cocktail, 1mM PMSF, and 1 Mm sodiumorthovanadate.) was added into the wells in order to dislodge the cells from the plate. Then by using the scraper, cells are collected and put into the eppendorfs. Then collected cells were sonicated for about 9 seconds. Then, supernatant was transferred into new eppendorfs and they were placed at -80°C as the loading of the samples and Lowry assay was performed in order to calculate the necessary amount of the protein from each tubes.

3.5.2. Lowry Assay

BSA standards were prepared from the range within 0.05-0.75 to plot a standard curve. Protein content was determined by adding one microliter of sample and 4 microliter of dH₂O into 96 well plate as duplicate. Bio-Rad Lowry assay was used, 25 μ l of reagent A, 200 μ l of reagent B and samples were mixed and incubated 15 minutes. After incubation, absorbance values were measured at 750 nm using ELISA Microplate reader.

3.5.3. Sodium Dodecyl Sulfate-Polyacrylamide Gel Electrophoresis (SDS-PAGE)

SDS-PAGE method was applied for the separation of denatured proteins according to their molecular weight. 15% separating gel and 4% stacking gel was prepared as shown on the table below.

Table 3.5. The ingredients of separating and stacking gel

	Stacking Gel	Separating Gel
Stock solutions	4 percent	15 percent
30 per cent (w/v) acrylamide / 0.8 per cent bisacrylamide	0.65 ml	7.5ml
0.5 M Tris-HCl containing 0.4 per cent (w/v) SDS, pH 6.8	1.25 ml	
1.5 M Tris-HCl containing 0.4 per cent (w/v) SDS, pH 8.8		3.75 ml
dH ₂ O	3.05 ml	3.75 ml
10 per cent (w/v) APS	25 μ l	50 μ l
TEMED	5 μ l	10 μ l

Separating gel was mixed gently and the gel was poured from edge of the glass until the level is equal to the green bar holding the glass plates. The rest was filled with isopropanol in order to prevent the air contact. Following the polymerization, isopropanol was removed by washing with water until isopropanol was finely removed. Stacking gel was mixed

gently and poured from edge of the glass. The comb was inserted yet it is important to ensure that there are no air bubbles and waited until the gel was solidified. After preparing the gel, samples are loaded according to the calculated volume and 2X Laemmli buffer (2X Laemmli buffer which includes 125 mM Tris-HCl, pH 6.8, 20% (v/v) glycerol, 4% (v/v) SDS, 10% (v/v) 2- β -mercaptoethanol and 0.004% bromophenol blue) was added with the 1:1 ratio of prepared solution. 2 μ l of protein ladder marker was added into the first well. After loading these samples the first 10 minutes samples were ran at 90 volts then voltage was increased at 120V. SDS-PAGE was performed with Bio-Rad Mini-PROTEAN Tetra cell Electrophoresis System.

3.5.4. Western Blotting

For the wet-dry transfer process, sandwich method was applied. Proteins on the gel were then transferred to the nitrocellulose membrane (0.22 μ m and 0.45 μ m). Membrane, sponges and Whatmann papers were moistened with cold running buffer pH: 8.3 (25 mM Tris-Base, 192 mM glycine and 20 per cent (v/v) methanol) before western blotting was performed. Gel Sandwich was prepared as black side of cassette, sponge, Whatmann paper, gel, nitrocellulose membrane, Whatmann paper and sponge. The sandwich cassette was placed into the holder that the membrane was sided to the anode and the gel sided to the cathode. The cassette holder was then put into the transfer tank which was filled with the cold transfer buffer and put the tank on the ice box to prevent overheating during the transfer process. The transfer was performed at 220mA for 1 hour. While transferring process 5% of non-fat milk blocking solution is prepared in 1X TBS-T. Then, transferred membrane is blocked for 1 hour in a milk solution. Later, TRAIL and BIK antibodies with a 1:200 dilution were prepared in 3% of BSA and membrane was incubated overnight in the cold room. The following day, incubated membrane was washed three times with TBS-Tween solution pH 7.4 for 5 minutes and then blocked with milk solution for 20 minutes. While blocking process secondary antibody was prepared in 10 ml of milk solution with 1:5000 dilutions (anti-mouse IgG and anti-rabbit IgG). After giving the secondary antibody, membrane was shake for 1 hour. Another washing process of three times was performed with 1X TBS-T for three times and membrane was put into 1X PBS solution for 10 minutes. 10 minutes later, development of membrane, visualization process was performed. First membrane was incubated for 2 minutes in ECL-Amersham Imaging

Solution and then membrane is visualized using Bio-Rad Molecular Imager ChemiDoc XRS+ in order to see the bands of the trail and BIKDDA. Visualization process was performed in the time interval of 1 to 300 minutes.

3.6 SYNTHESIS AND CHARACTERIZATION OF PEPTIDES TARGETTING PROSTATE CANCER

3.6.1. Synthesis of Peptide

Peptide 562, Peptide 563 and Peptide 564 tagged with 5, 6-TAMRA and was synthesized by Bio peptide company. The sequences of peptides are listed as shown in Table 3.6.1.

Table 3.6. The sequence of the peptides

Names of the Peptides	Sequence
Peptide 562	Tamra-SHSFSVGS GDHSPFT-OH
Peptide 563	Tamra-GRFLTGGTGRLLRIS-OH
Peptide 564	Tamra-LSFFSCWLRRSFSLT-OH

3.6.2. Determination of Peptide Binding Affinity by Flow Cytometry

300,000 cells/well were seeded onto 6 well plates for 22RV1, PNT1A, LNCAP and HUVEC cell lines. Following day, 10 μM (10^{-5}mol/L) of each of the three TAMRA-labeled peptides were added onto each well with serum free medium and incubated 1 hour. After incubation, cells were collected and fixed with 0.5% formaldehyde. The binding affinity of peptides was analyzed by flow cytometer.

3.6.3. Determination of Peptide Binding Affinity by Confocal Microscopy

50,000 cells for each cell line were seeded onto eight-well chamber and incubated at 37 °C for 24 h. Peptides were solved in serum free fresh media with the concentration of 10 µM. Peptide media mix were added onto each well and incubated for an hour at 37 °C. After incubation, cells were washed three times with serum free media. After washing step, cells were fixed with 2% formaldehyde solution on ice for 20 minutes. Formaldehyde was removed through washing with serum free media for three times. 1 drop of DAPI was added onto the coverslip and incubated for 5 minutes to stain the nucleus. To remove DAPI fixed cells were washed with PBS twice. The cells were imaged under confocal microscopy.

3.7. DETERMINATION OF CELL DEATH

3.7.1. Trypan Blue Assay

22RV1 cells were seeded into a 6-well plate (30×10^4 cells/well), after 24h transfections were carried out with BIKDDA, Trail and C3 plasmid with using Xtreme Gene HP DNA transcription reagent, in Opti-MEM according to the instructions. 1:3 ratios of DNA:Transfection reagent were performed.

After transfection trypan blue assay was performed at 24h, 48h and 72h time points. Medium was taken and cells were washed with PBS. Cells were trypsinized and collected. Cell suspensions were centrifuged at 1500 rpm 5 min. Pellet was solved in 1ml PBS. 90 microliter cell-PBS suspension and 10 microliter of trypan blue was mixed and counted with hemocytometer.

3.7.2. Annexin V

22RV1 cells were seeded into a 6-well plate (30×10^4 cells/well), after 24h transfections were carried out with BIKDDA and C3 plasmid with using Xtreme Gene HP DNA transcription reagent, in Opti-MEM according to the instructions. 1:3 ratios of DNA:Transfection reagent were performed. Transfected cells were incubated 72h at 37C.

After incubation, cell media was collected and cell monolayer was washed with PBS. Cells were dislodged with trypsin and collected. Supernatant was removed and pellet was washed with 1 ml PBS for 5 minutes. After washing step, 300 micro liter of Annexin binding buffer was added onto the cell pellet. 5 microliter of Annexin V PE conjugated antibody was added and incubated 20 minutes on ice. 1microliter of PI antibody was added just before performing flow cytometry. Annexin V method was performed to observe apoptosis by using FL2 Laser, red and Necrosis was determined with PI antibody by FL2 laser, red at flow cytometer.

3.8. THE CYTOTOXICITY OF POLYMERSOME POLYMER AND FORMULATION

Since the PetOx5900-b-PCL4200 polymer can be dissolved in DMSO at a concentration of 150 mg / ml, the highest concentration to be used for the polymersome and polymersome formulation was determined to be 150µg/ml. HDF, HFOB1.19, HEPG2 and PNT1A cells were plated into 96 micro culture well plates at a density of 2500 cells/well and incubated overnight at 37 ° C in an atmosphere containing 5% carbon dioxide. The following day polymersome polymer and polymersome formulation were added at various concentrations, 25µl/ml, 50µl/ml, 75µl/ml, 100µl/ml and 150µl/ml and incubated for 24, 48 and 72h. The toxic effect of DMSO alone was measured by growing cells in growth medium containing 0.001 per cent DMSO. Cytotoxic effect was then assessed by WST1 assay, which was performed according to the manufacturer's instructions. The percentage of cell viability was calculated by assigning the absorbance value obtained from non-treated cells as 100 per cent.

4. RESULTS

4.1. SITE-DIRECTED MUTAGENESIS OF BIKDD TO BIKDDA

TRAIL and the mutant form of BIK gene, BIKDDA was used as pro-apoptotic genes to transfect the model prostate cancer cell lines and induce apoptosis. Although peGFP-TRAIL was commercially available, BIKDDA plasmid was not therefore site directed mutagenesis was performed on pEGFP-BIKDD plasmid (Section 3.2.1) to generate pUK21 plasmid carrying the mutant BIKDDA gene.

BIKDDA gene sequence analysis using next gen sequencing showed that the codon ACC was changed as GCC both in the negative and positive stand, which is translated into protein as conversion of 124th serine (D) amino acid to alanine amino acid (A) (Fig.4.1.).

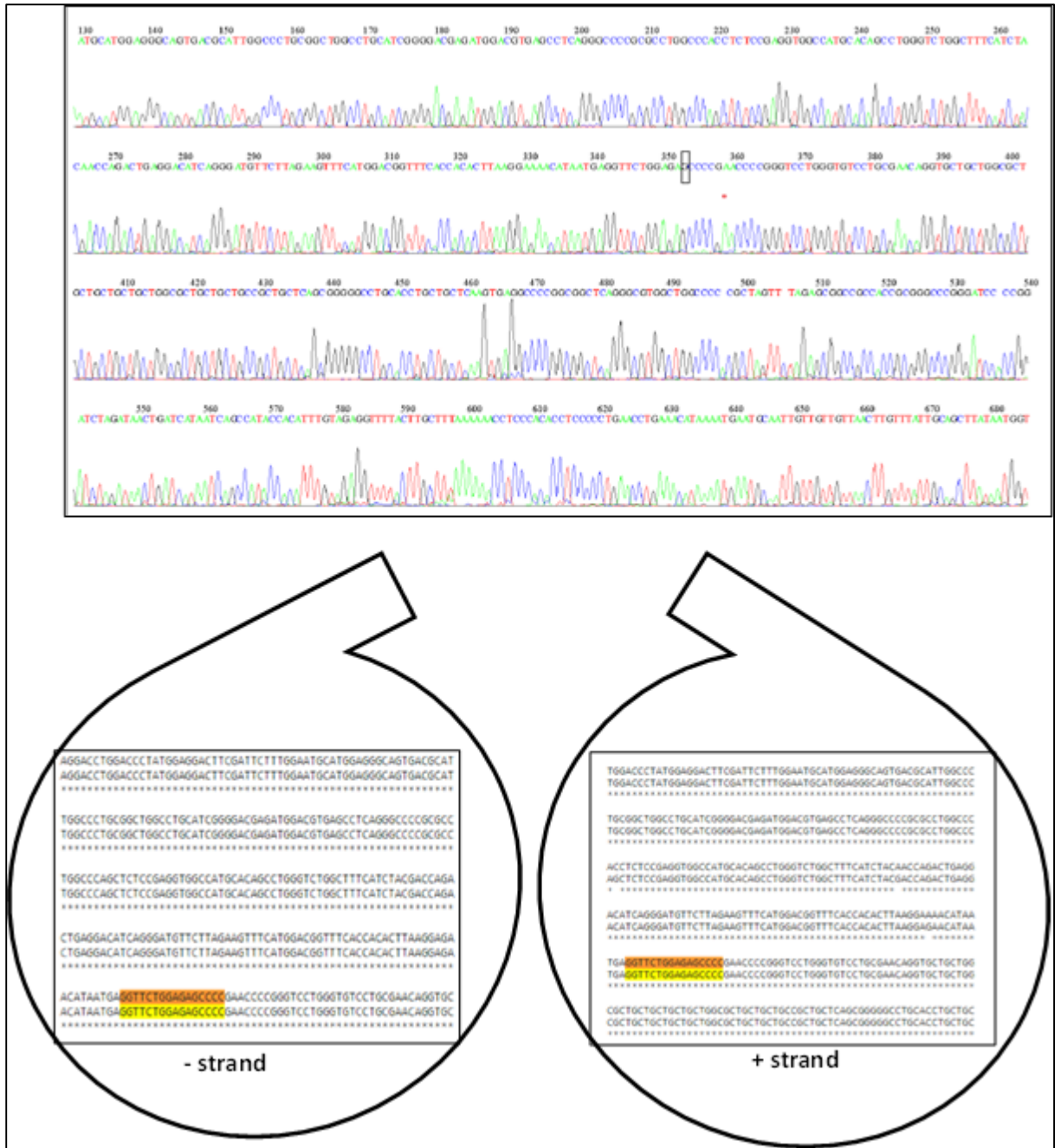


Figure 4.1. The Chromatogram result of the site directed mutagenesis

4.2. DETERMINATION OF THE TRANSFECTION EFFICIENCY OF PEGFP-TRAIL AND PEGFP-BIKDDA ON 22RV1 CELLS USING THE X-TREMEGENE TRANSFECTION REAGENT

In order to optimize the transfection conditions, 22RV1 cells were transfected with pEGFP-TRAIL and pEGFP-BIKDDA genes at 24, 48 and 72 hours using 1:1, 2:1, 1:3 DNA to transfection reagent ratios (Section 3.3.1). Analysis of images captured at the three different time points indicated that the highest transfection efficiency was achieved when 22RV1 cells were transfected using 1:3 DNA to X-tremeGENE ratio after 48 hours incubation both for BIKDDA and TRAIL.

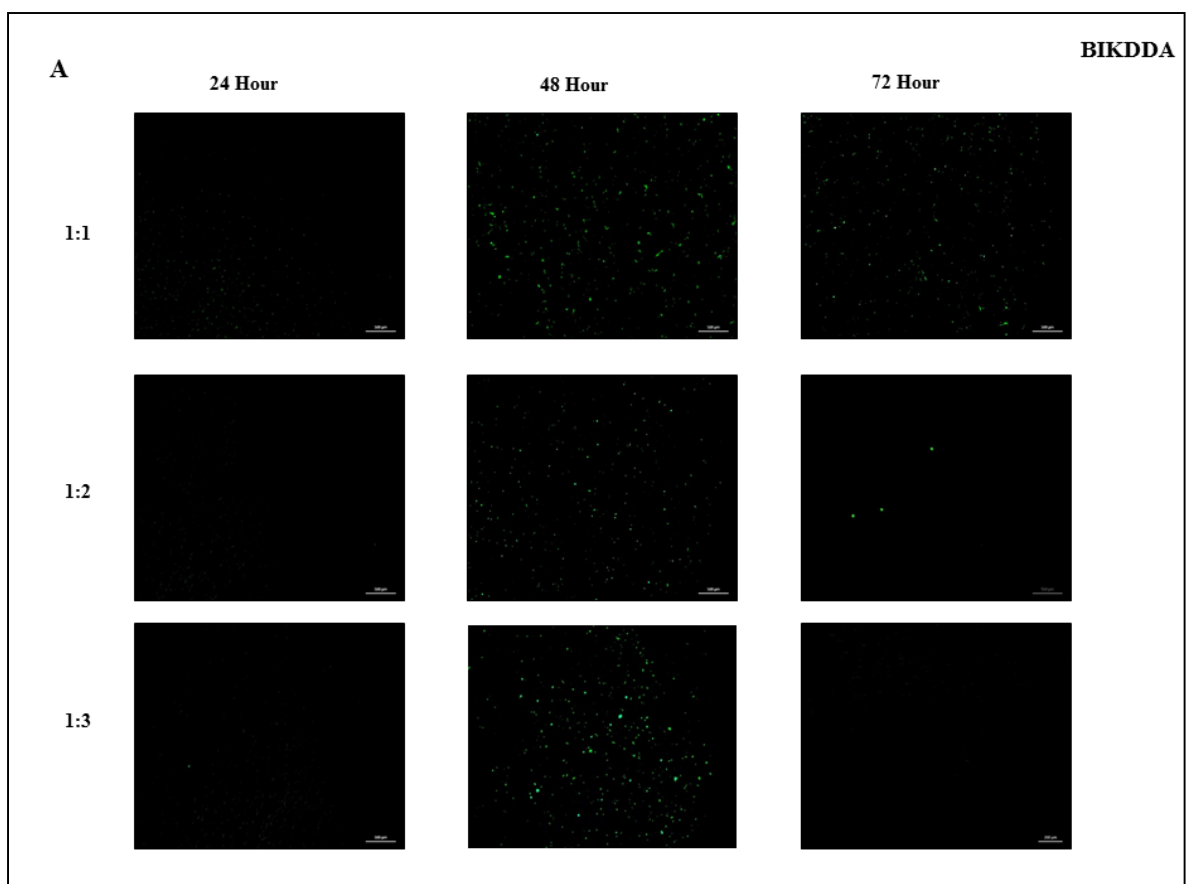


Figure 4.2. 22RV1 cells were transfected with pEGFP-BIKDDA by X-tremeGENE HP DNA transcription reagent using 1:1, 1:2 and 1:3 ratios of DNA:Transfection reagent ratio. Images were taken with a 5x objective under a fluorescent microscope at 24, 48 and 72 hours after transfection. The results are representative of three independent experiments.

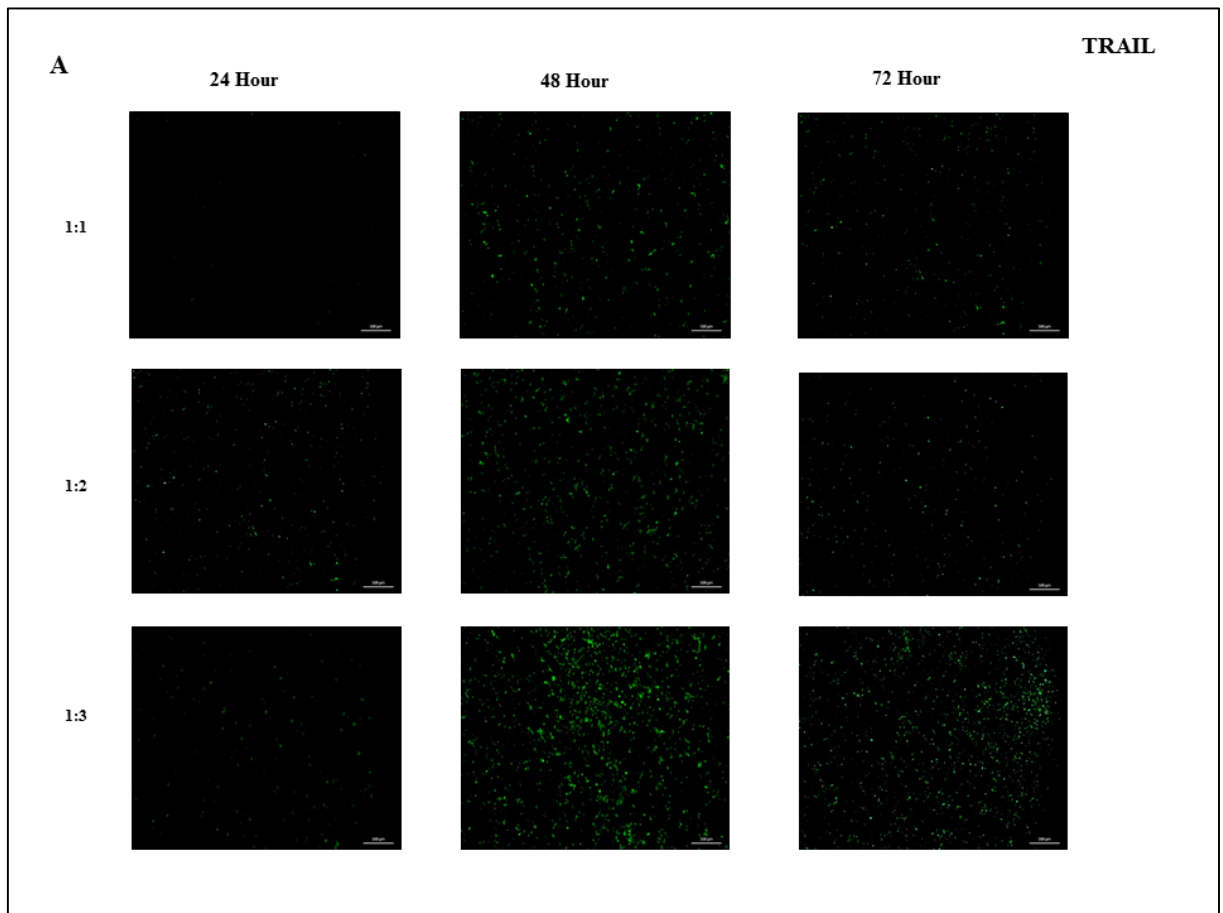


Figure 4.3. 22RV1 cells were transfected with pEGFP-TRAIL by X-tremeGENE HP DNAtranscription reagent using 1:1, 1:2 and 1:3 ratios of DNA:Transfection reagent ratio. Images were taken with a 5x objective under a fluorescent microscope at 24, 48 and 72 hours after transfection. The results are representative of three independent experiments.

As can be seen from Figure 4.2., 1:1 DNA to X-tremeGENE ratio positively stained only nine per cent cells at 24 hours while at 48 and 72 hours average percentage of GFP positive cells was increased to 14 per cent and 13.2 per cent, respectively. Similarly, 1:2 DNA to X-tremeGENE ratio also gave a low transfection efficiency with eight per cent cells at 24 hours, 10 per cent cells at 48 hours and 6.9 per cent of cells at 72 hours. The highest transfection efficiency achieved with 1:3 DNA to X-tremeGENE ratio resulted in 22 per cent of GFP positive cells at 48 hours, while nine per cent and 8.2 per cent of GFP-positive cells was recorded at 24 and 72 hours, respectively.

When the images taken for pEGFP-TRAIL transfection efficiency was evaluated, it was seen that 1:1 and 1:2 DNA to X-tremeGENE ratio gave an average number of 12 per cent

GFP expression at 24 hours, while this number was increased by 2.6 fold when the incubation time was increased to 48 and 72 hours. As expected when 22RV1 cells was transfected with 1:3 pEGFP-TRAIL to X-tremeGENE ratio, the average percentage of GFP positive cell expression was 10 per cent, 24 per cent and 13 per cent at 24, 48 and 72 hours.

4.3. GENE EXPRESSION LEVEL OF BIK AND TRAIL IN 22RV1 CELL LINE

In order to investigate the mRNA expression levels of TRAIL and BIK in 22RV1, cells were seeded into 6 well plates (Section 3.3.) and transfected using the X-tremeGENE reagent as mentioned above. After transfection, RNA isolation was performed and TRAIL and BIKDDA gene expression levels were determined by qPCR method as described at Section. 3.4.

As stated in Figure. 4.4., BIK mRNA levels in 22RV1 cells transfected with BIKDDA was found to be increased by 1.6-fold in comparison to non-transfected control cells after 24 hours. At the end of 48 hours, BIK gene expression level was found to be 12.5 fold more when compared to non-transfected control 22RV1 cells. The highest level of BIK mRNA expression was obtained at the end of 72 hours of incubation.

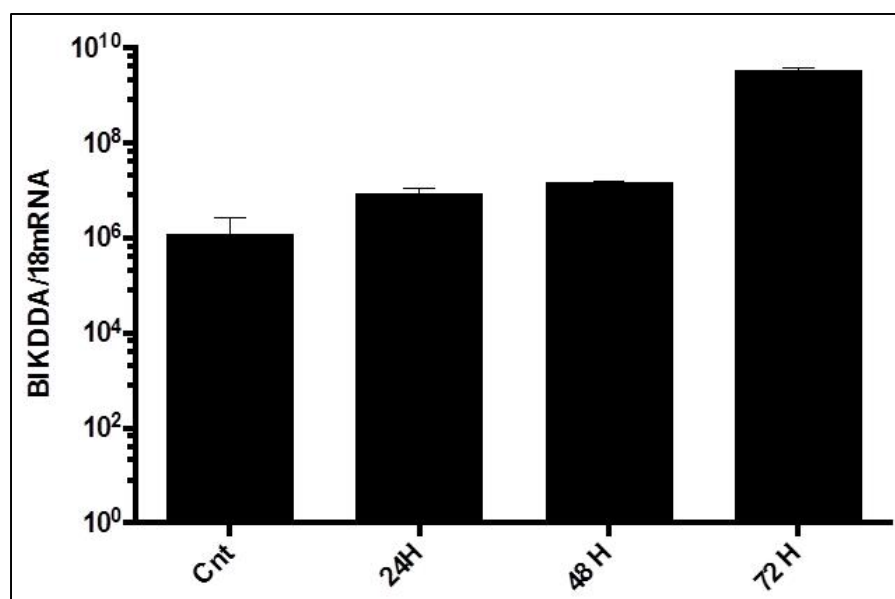


Figure 4.4. BIK mRNA levels were analyzed using qPCR in BIKDDA transfected and non-transfected (Cnt) 22RV1 cells. BIK gene expression levels were normalized against that of 18s RNA.

During the course of the experimental process, it was observed that 22RV1 cells showed initial signs of cell death after 24 hours and most of the cells entered apoptosis after 72 hours. Conclusively, the TRAIL expression was found to be 3.6 times higher in transfected 22RV1 cells than their control counterparts at 24 hours. In the transfected cells, TRAIL expression at 48 hours was the highest, interestingly a decrease in TRAIL mRNA expression was recorded at 72 hours. (Fig. 4.5.)

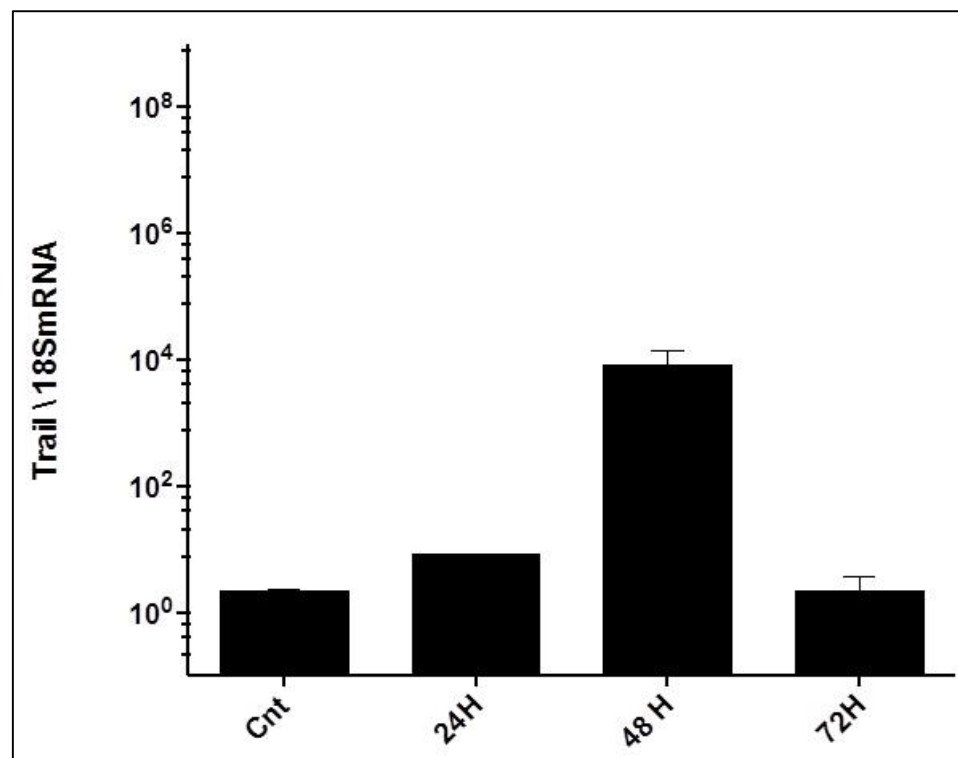


Figure 4.5. TRAIL transfected and untreated (Cnt) 22RV1 cells was evaluated using qPCR, TRAIL mRNA levels were normalized against 18s RNA expression levels.

4.4. PROTEIN EXPRESSION LEVEL OF BIKDDA AND TRAIL IN 22RV1 CELL LINE

The protein expression levels of BIKDDA and TRAIL in 22RV1, prostate cancer cell line, were analyzed by Western Blot analysis as mentioned before in Material and Method Chapter 3.5. Cell lysates were collected and used for the detection of protein expression level of BIK and TRAIL. β -actin was used to control the protein loading in each sample.

As shown in Figure 4.6., Following the transfection, BIK expression level was found to be 37 per cent higher in comparison with non-transfected control cell. Similarly, TRAIL expression level was found to be six per cent higher in the 22RV1 transfected with TRAIL compared to the non-transfected control cells.

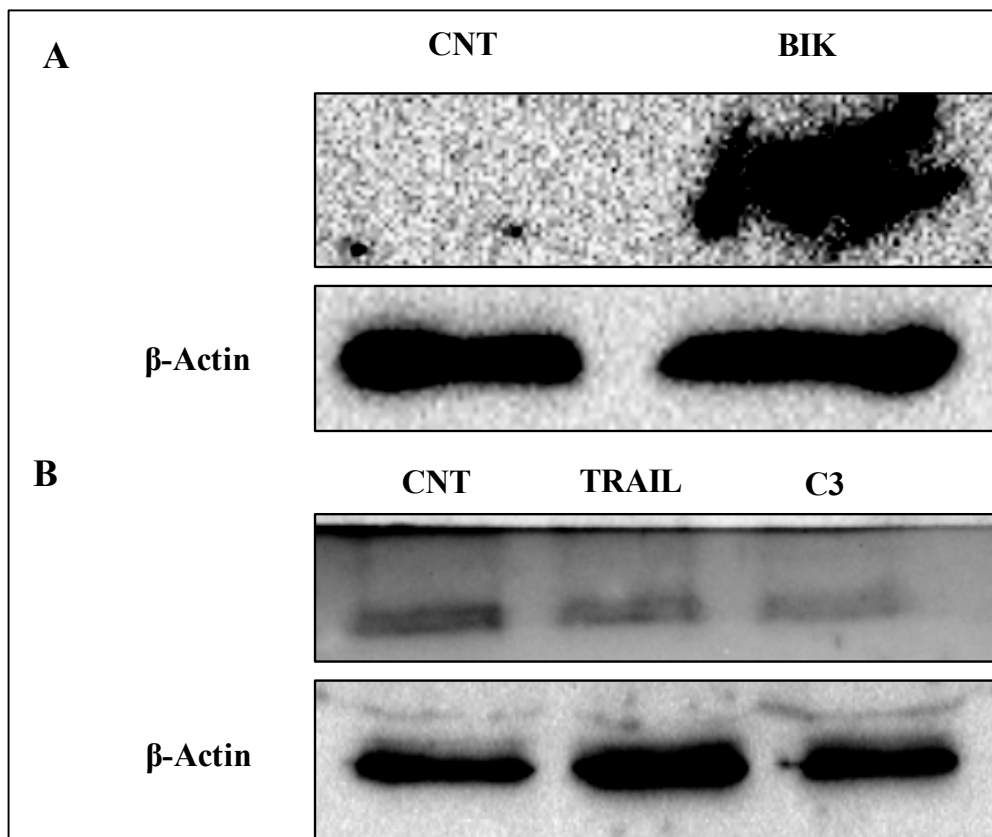


Figure 4.6. Western Blot analysis proteins in non-transfected (CNT), (A) Bik and (B) TRAIL transfected, and mock vector transfected (pEGF-c3) 22RV1 Cell Lines. Rabbit polyclonal anti-BIK rabbit monoclonal antibody (1:500 dilutions) was used to detect BIK protein expression (A) and anti-TRAIL mouse monoclonal antibody (1:1000 dilution) was used to detect TRAIL expression (B). For the detection of β -actin, mouse monoclonal anti β -actin (1:5000 dilutions) was used. Protein bands were imaged by Chemi doc. Image Lab

Program described in Section 3.5.4

4.5. EFFECT OF PRO-APOPTOTIC GENE EXPRESSION ON THE CELL VIABILITY

Since 22RV1 cells were defined as TRAIL-resistant, we wanted to compare the apoptosis inducing efficiencies of TRAIL and BIKDDA in 22RV1 cells. In order to determine and compare the lethal effect of pro-apoptotic BIKDDA and TRAIL ligand genes on 22RV1 cells, 22RV1 cells were stained with trypan blue as mentioned at Section 3.7.1 and cell viability was measured by counting the dead (stained with blue) and alive cells under phase-contrast microscope.

BIKDDA transfection resulted in an average of 70 per cent cell death in the 22RV1 cells at 24, 48 and 72 hours (Figure 4.7.) while TRAIL transfected 22RV1 cells displayed only 50 per cent cell death at all three time points. Non-transfected 22RV1 cells and cells transfected with empty vector backbone pEGFP-C3 has shown 10 per cent residual cell death indicating that the transfection protocol itself did not have a false negative effect on the cell viability. Taken together, BIKDDA transfection had more apoptotic effect than TRAIL in 22Rv1 cells.

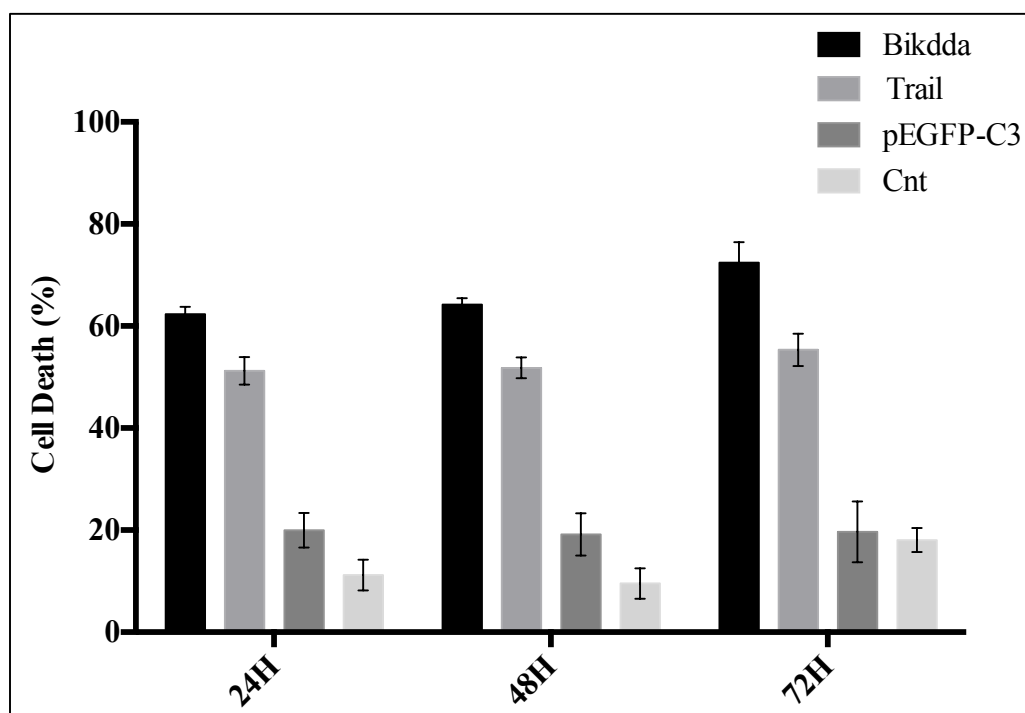


Figure 4.7. Effect of Pro-apoptotic gene transfection on the cell viability of 22RV1 cells. A trypan blue assay was then used to measure cell viability.

4.6. DETECTION OF APOPTOSIS BY ANNEXIN V STAINING

To assess whether BIKDDA transfection resulted in induction of apoptosis in 22RV1 cells, cells transfected with BIKDDA as mentioned at Section 3.3 were stained with Annexin V PE conjugated as described in Section 3.5.2 Annexin V is a protein which has a higher affinity for the phospholipid phosphatidylserine in cells undergoing apoptosis.

As shown in Figure 4.8, the apoptotic rate of untreated 22RV1 cells was 0.03 per cent, while cells treated with the well-known apoptotic inducer, staurosporine, was detected as 34.56 per cent. Cells transfected with BIKDDA showed 40.17 per cent cell death and the percentage of cells undergoing apoptosis was analyzed as 12.19 per cent in cells transfected with C3, null plasmid. Taken together the results of Annexin V experiment, showed that the transfection of 22RV1 cells BIKDDA resulted in a high apoptosis level similar to the well-known apoptotic inducer, staurosporine.

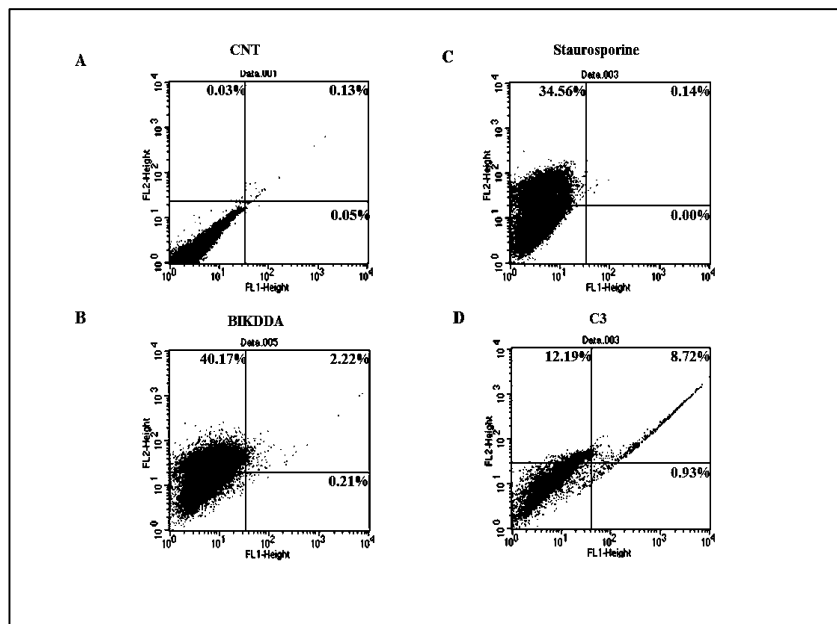


Figure 4.8. The Annexin V staining on BIKDDA transfected 22RV1 cells. The upper left quadrant of representative histograms indicates cells apoptotic cells that are positively stained with PE conjugated Annexin V. **A.** The apoptotic rate of control **B.** The apoptotic rate of cells transfected with BIKDDA with 1:3 ratio Extremegene:DNA **C.** The apoptotic rate of cells treated with staurosporine, the well-known apoptotic inducer **D.** The apoptotic rate of cells transfected with C3 null plasmid with 1:1 ratio Extremegene:DNA

4.7. ANALYSIS OF CELLULAR CYTOTOXICITY FOR NANOCARRIERS

In order to detect the cytotoxic effect of PetOx-based polymer and their polymersome formulations, HEPG2, HDF, Hfob1.19 and PNT1A cells were and the cell cytotoxicity was then measured by WST1 assay, which was performed according to the manufacturer's instructions as described Section 3.6. The percentage of cell viability was calculated by assigning the absorbance value obtained from the non-treated cells as 100%.

Figure 4.9, showing the viability rates of HDF cells after 96 hours of incubation indicates that the PetOx5900-b-PCL4200 polymer and its formulation increased the cell viability by 20-40% in HDF cells at 25, 50, 100 and 150 $\mu\text{g/ml}$ treatment concentrations. In order words, no cytotoxic effect was detected on cell proliferation was observed in HDF cells treated with the indicated concentrations of PetOx5900-b-PCL4200 polymer and polymersome.

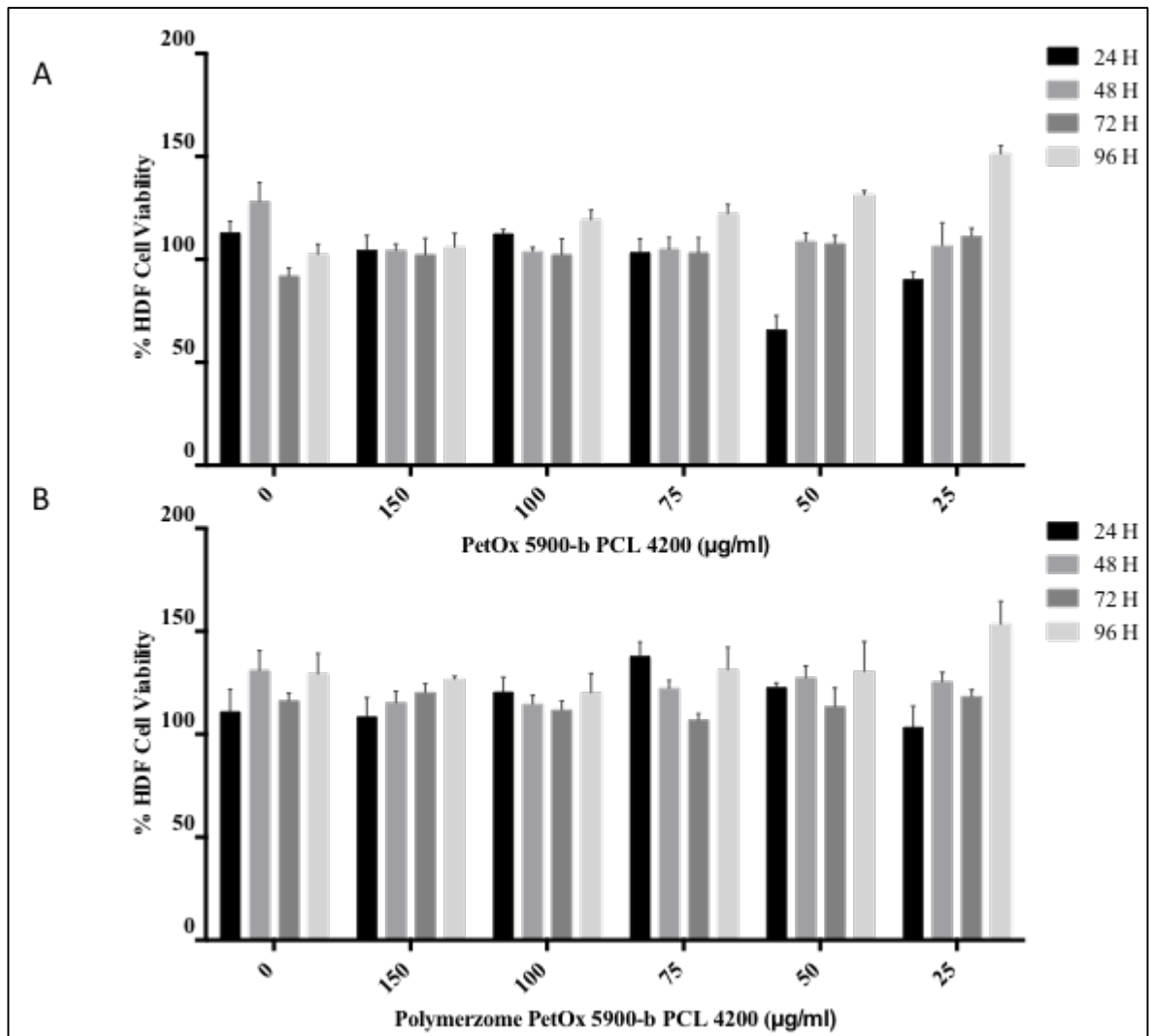


Figure 4.9. The cytotoxic efficacy of **A.** PetOx5900-b-PCL4200 polymer and **B.** PetOx5900-b-PCL4200 polymersome formulation on the primary human dermal fibroblast cells (HDF). Each data point represents the mean percentage of viable cells at different time points treated with three different concentrations (25-150µl/ml) of at least three separate experiments performed in triplicate.

As shown in Figure 4.10., the treatment of PNT1A cells with PetOx5900-b-PCL4200 polymer resulted in a 10 per cent decrease in the cell proliferation at all concentrations for the four time points tested. However, it has been observed that the polymersome formulation does not cause any toxicity on PNT1A viability and additionally led to a 10-20 per cent increased cell proliferation rate in PNT1A cells at all the doses tested.

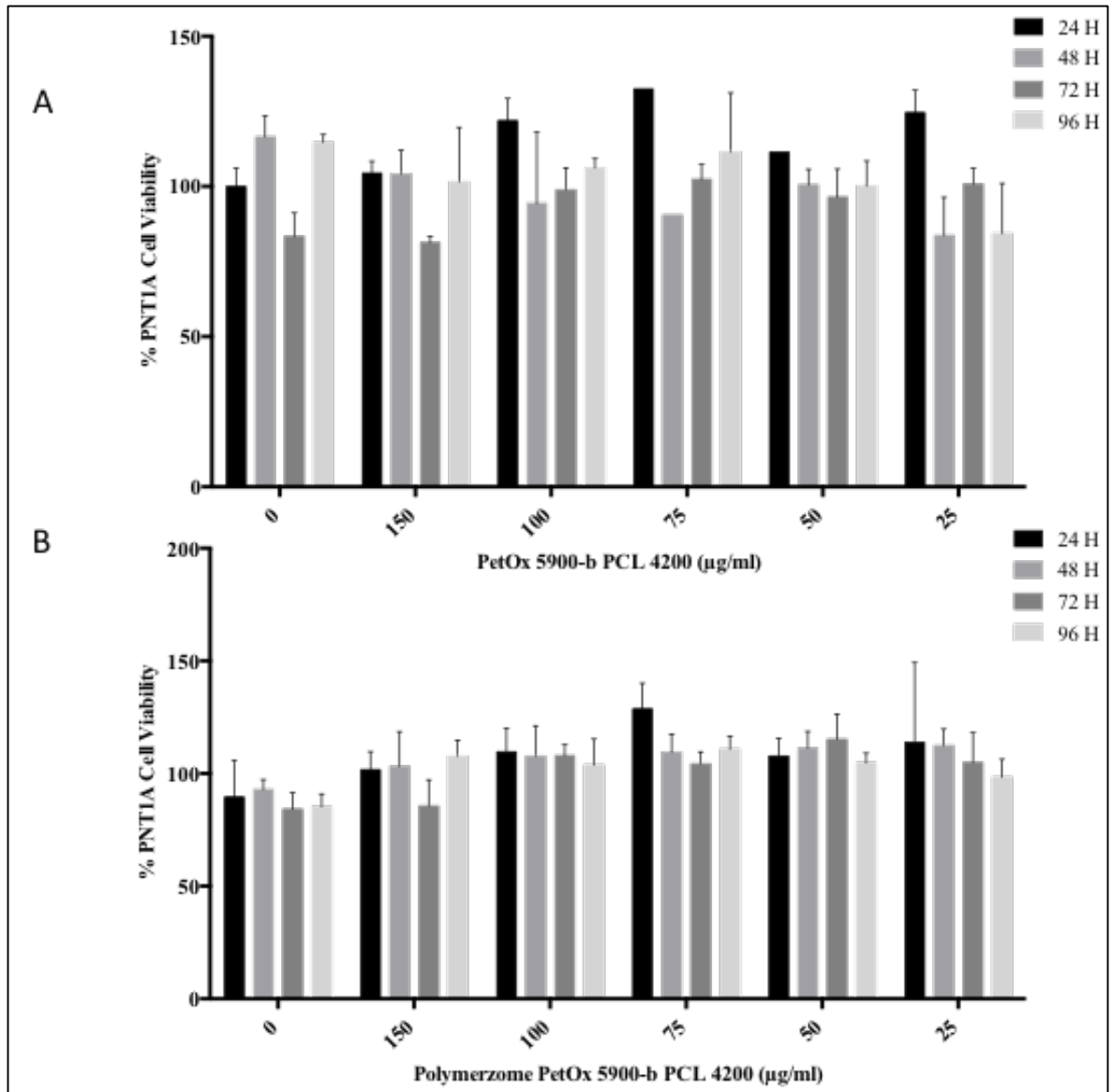


Figure 4.10. The cytotoxic efficacy of A. PetOx5900-b-PCL4200 polymer and B. PetOx5900-b-PCL4200 polymersome formulation on the healthy prostate epithelium immortalized cell line PNT1A. Each data point represents the mean percentage of viable cells at different time points treated with three different concentrations (25-150µl/ml) of at least three separate experiments performed in triplicate.

For HEPG2 cell line, PetOx5900-b-PCL4200 polymer displayed a slight toxicity with a 20 per cent at the 50µl/ml, 75µl/ml, 100µl/ml and 150µl/ml, while no decrease in HEPG2 cell viability was detected at 25µl/ml for 48 and 72 hours. Interestingly, there was no remarkable toxic effect for this polymer at 24 hours at all doses tested. Exposure of HEPG2 cells to PetOx5900-b-PCL4200 polymersome at 50µl/ml, 75µl/ml, 100µl/ml and

150 μ l/ml resulted in an approximate 30 per cent toxicity at 72 and 96 hours, albeit no detectable toxic effect was evident at 24 and 48 hours (Figure 4.11.).

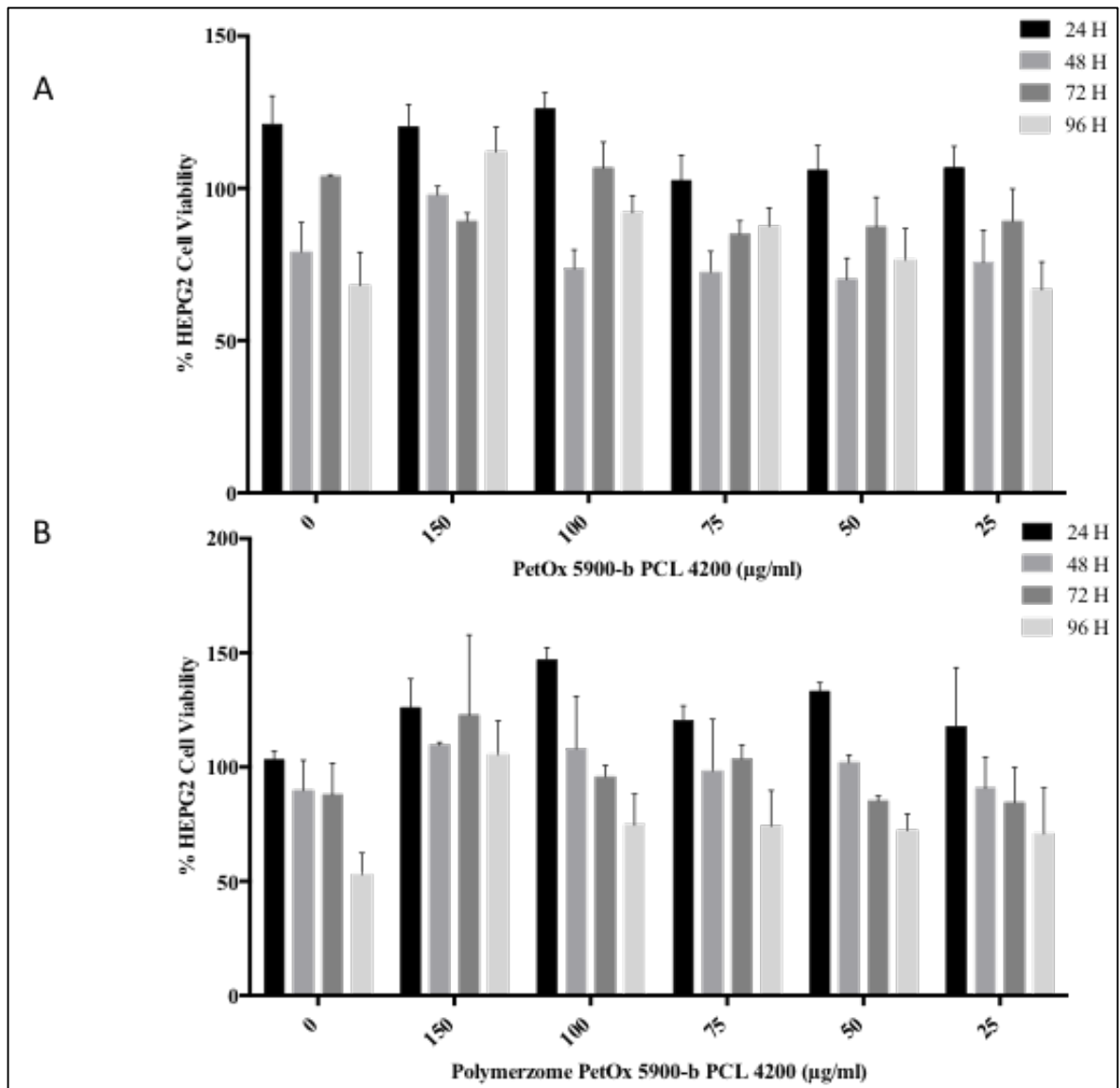


Figure 4.11. The cytotoxic efficacy of A. PetOx5900-b-PCL4200 polymer and B. PetOx5900-b-PCL4200 polymersome formulation on the healthy liver hepatocellular cell line HEPG2. Each data point represents the mean percentage of viable cells at different time points treated with three different concentrations (25-150 μ l/ml) of at least three separate experiments performed in triplicate.

When the effect of the PetOx5900-b-PCL4200 polymer on Hfob 1.19 cell viability was examined, there was a 10 per cent decrease in cell viability at 24 hours at all doses tested. Similarly, there was no significant cytotoxicity detected for this polymer at 72 and 96

hours for all doses tested whereas, 10-20 per cent increase in cell proliferation was detected for the 50 μ l/ml, 75 μ l/ml, 100 μ l/ml and 150 μ l/ml concentrations at 48 hours. Treatment of these osteoblasts with the polymersome formulation did not cause any significant change in the percentage of viable cells at 24 and 72 hours, interestingly an average of 20 per cent decrease in cell viability was recorded at all doses tested at 48 and 72 hours.

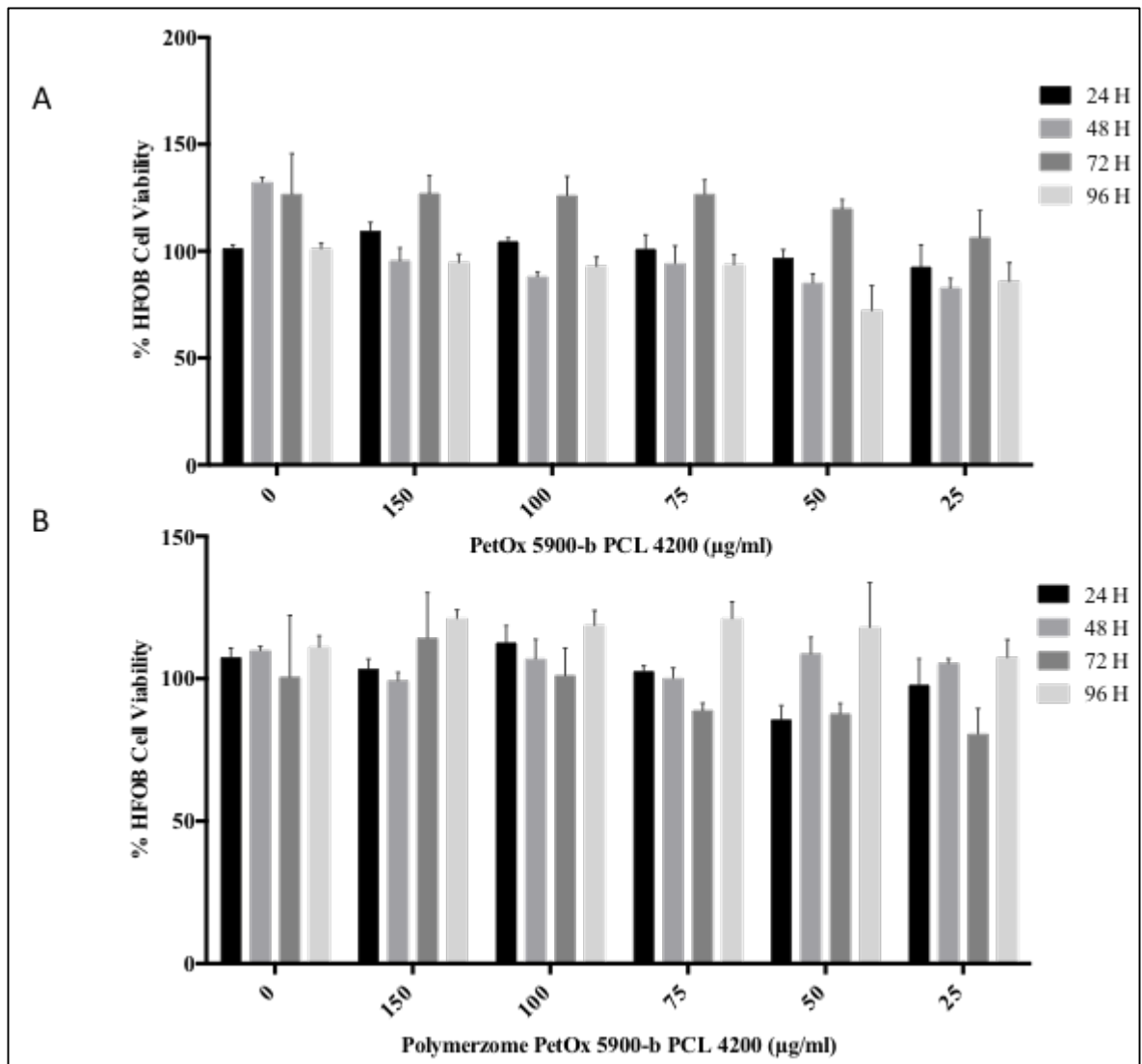


Figure 4.12. The cytotoxic efficacy of A. PetOx5900-b-PCL4200 polymer and B. PetOx5900-b-PCL4200 polymersome formulation on the human fetal osteoblastic cell line Hfob 1.19.

4.8. POLYMERSOME DELIVERY OF BIKDDA TO 22RV1 CELLS

In order to determine the delivery efficiency of PetOx5900-b-PCL4200 polymersome carrying BIKDDA (PSm-BIKDDA) gene on 22RV1 cell line, 22RV1 cells were incubated with 1.12 $\mu\text{g}/\text{ml}$ of PSm-BIKDDA (2 μg DNA/ 10^6 cells) as previously described in Section 3.3.

As shown below in Figure 4.13., the fluorescence imaging of cells revealed 42.4 per cent transfection efficiency of PSm-BIKDDA for 22RV1 cells.

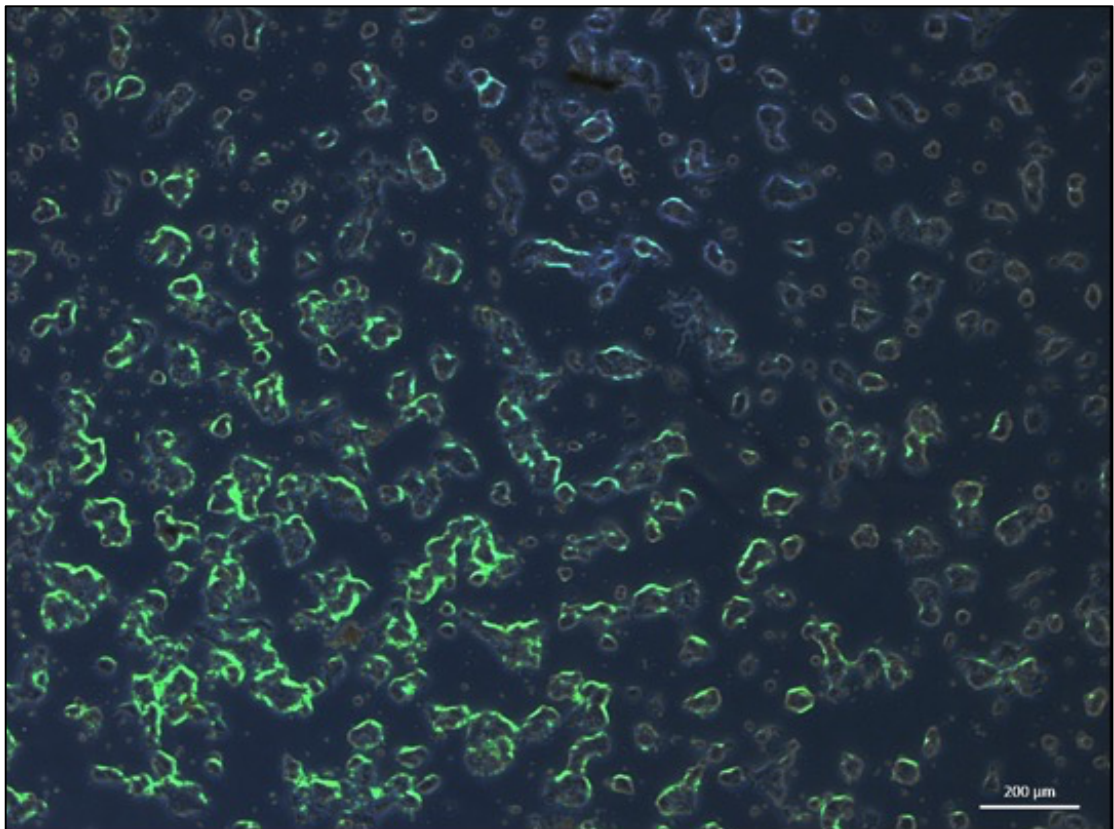


Figure 4.13. 22RV1 cells were incubated with PSm-BIKDDA for 24 hours (A). Representative image was taken on a fluorescent microscope using 5 x objective . Bar, 200 μm

As PSm-BIKDDA led to cellular toxicity after 24 hours, 22RV1 cells incubated with the BIKDDA loaded polymersome for 24 hours were analyzed for the BIK mRNA level. QPCR analysis revealed a 4.5-fold increase in BIK mRNA levels in PSm-BIKDDA treated 22RV1 cells when compared to cells treated with non-treated 22RV1 cells (Figure 4.14.).

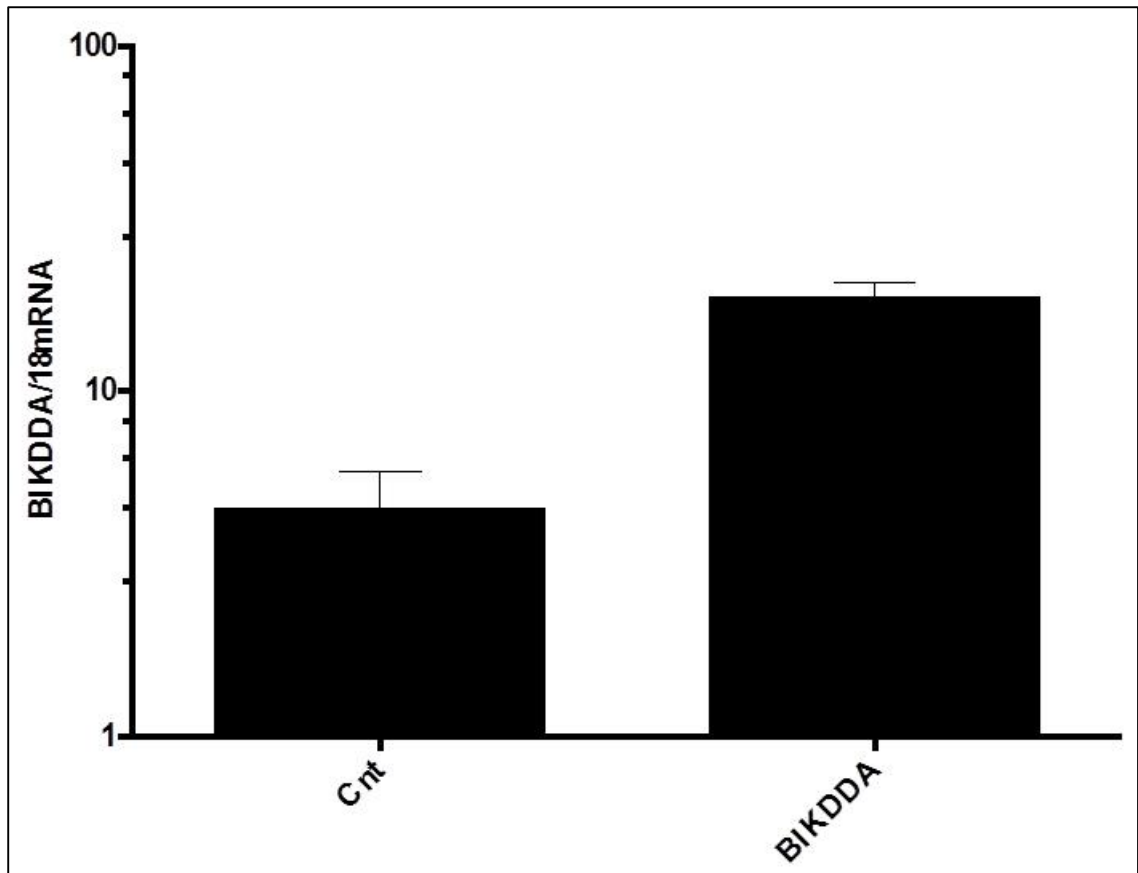


Figure 4.14. Polymersome encapsulated BIKDDA transfected and untreated (Cnt) 22rv1 cells was evaluated using qPCR, BIK mRNA levels were normalized against 18s RNA expression levels.

To assess whether 3PSm-BIKDDA treated 22RV1 cells resulted in the induction of apoptosis, Annexin V staining was applied as described in Section 3.7.2. In line with the previous experiments, BIKDDA expression mediated by the functionalized polymersome was capable of inducing cell death in 22RV1 prostate cancer cell line. As shown in Figure 4.15, the apoptotic rate in untreated 22RV1 cells was recorded as 0.53 per cent, while 22RV1 transfected with PSm-BIKDDA exhibited a 38.40 per cent apoptotic rate with a detectable 11.52 per cent necrosis and/or late apoptosis.

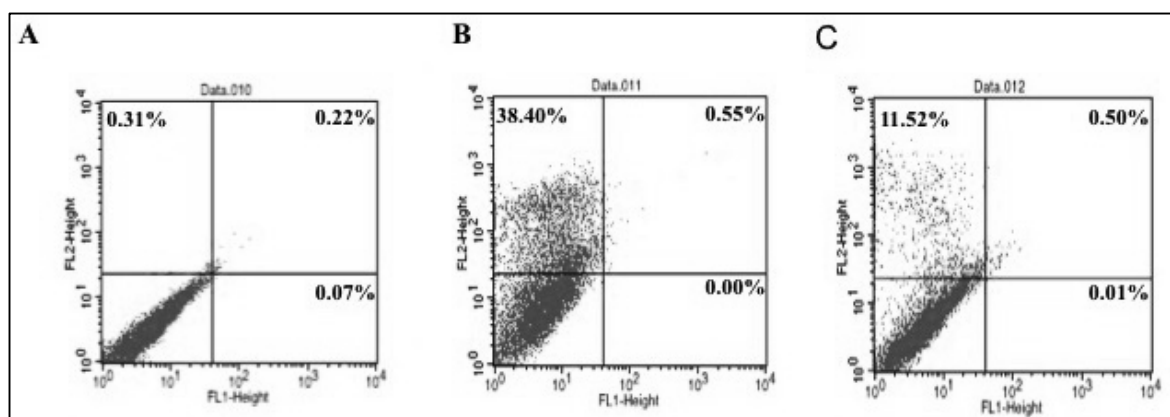


Figure 4.15. Annexin V staining of 22RV1 cells treated with PSm-BIKDDA polymersome. The upper left quadrant indicates cells undergoing apoptosis and positively stained with PE conjugated Annexin V. Histograms of Annexin V staining for non-treated (A) and PSm-BIKDDA treated 22RV1 cells stained with Annexin V (B) and propidium iodide (C) was presented.

4.9. BINDING AFFINITY OF PEPTIDE 562, PEPTIDE 563, AND PEPTIDE 564 TO PROSTATE CANCER AND HEALTHY CONTROL CELL LINES

To further address the specificity and affinity of the designed peptides P562, P563 and P564 toward PSMA, PSMA positive prostate cancer cell line 22RV1 and PSMA-negative healthy prostate cells PNT1A and human umbilical vein endothelial cell HUVEC were used as model. P562, P563 and P564 peptides conjugated with TAMRA were used at x concentration to treat all three cell lines for one hour and the binding affinity of these peptides to the cell surface of 22RV1, PNT1A and HUVEC was analyzed as described in Section 3.6.2.

Flow cytometry analysis of 22RV1, PNT1A and HUVEC for TAMRA staining showed that P563 displayed a low binding ability to PSMA negative or low PNT1A and HUVEC cells, while a high specific-binding was recorded for PSMA-positive 22RV1 (Fig 4.16., Table 4.16.).

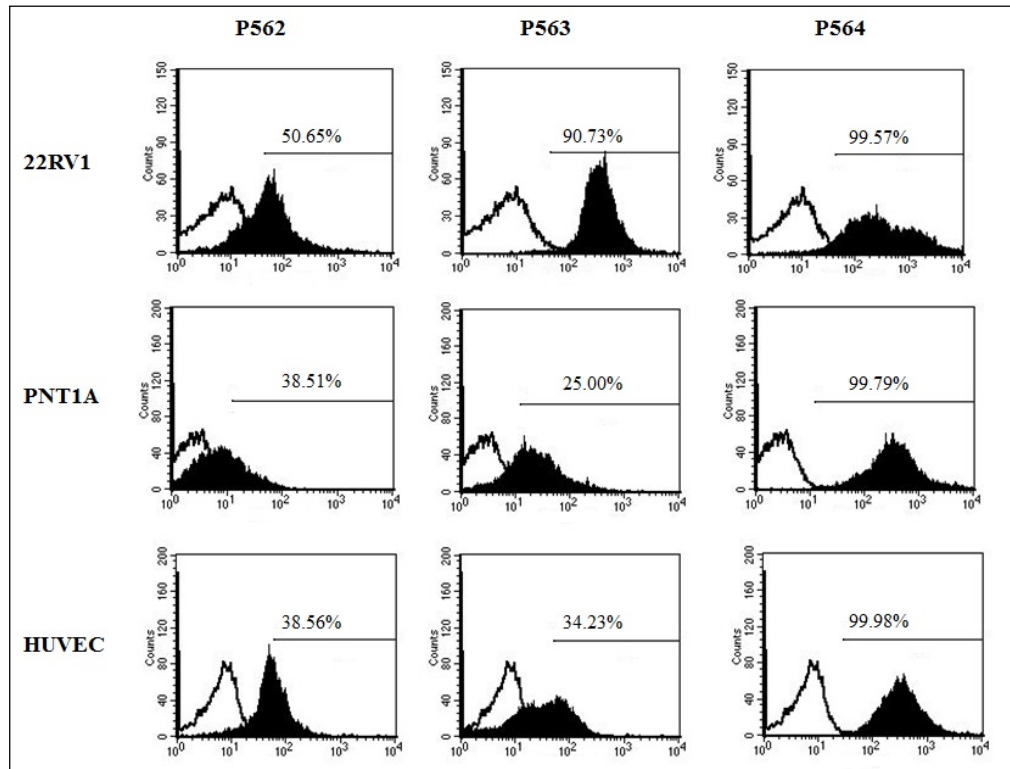


Figure 4.16. Representative histograms showing the binding activity of peptide 562 (P562), peptide 563 (P563) and peptide 564 (P564) to 22RV1, PNT1A and HUVEC. Cells were incubated with all peptides for 1 hour at 37°C and the fluorescent signal for TAMRA as the indication of peptide binding affinity was analyzed using Flow Cytometric Analysis as described Section 3.6.2.

Table 4.16. Average percentage of binding affinity recorded for the targeting peptides onto PNT1A, 22RV1 and HUVEC cells for three independent experiments.

Cell type/ Peptide	PNT1A	22RV1	HUVEC
P562	27.7%±5.01	48.3%±2.2	33.8%±6.7
P563	19.7%±4.9	93.7%±5.2	33.6%±6.9
P564	99.44%±0.7	99.9%±0.2	99.9%±0.01

As shown in Figure 4.16 and Table 4.16, P562 exhibited the lowest binding affinity for PNT1A, 22RV1 and HUVEC cell lines with the average percentage of 27.7 per cent, 48.3

per cent and 33.8 per cent, respectively. P564 showed the highest binding affinity among all three peptides to the cell trio (PNT1A, 22RV1 and HUVEC) with the percentage of 99.4 per cent, 99.9 per cent and 99.9 per cent, respectively suggesting an unspecific binding regardless of the PMSA antigen expression. On the other hand, P563 peptide showed a low binding affinity PNT1A with 19.7 per cent and HUVEC with 33.6 per cent, while 93.7 per cent of 22RV1 were found to be TAMRA-labeled when treated with this peptide.

Result of these experiments indicated that P563 was the only peptide that exhibited the specific binding to the PMSA-positive cell line 22RV1 cells and showed minimum nonspecific binding properties as its binding to PMSA-negative cells were at low percentage.

4.10. DETERMINATION OF BINDING AFFINITY OF PEPTIDES ON 22RV1 CELL LINE BY CONFOCAL MICROSCOPY

Confocal microscopy imaging was employed to monitor the binding affinity of P562, P563 and P564 to the control PNT1A and 22RV1 cells that were seeded at 5×10^4 density to 8-well chamber slides and allowed to attached for 24 hours prior to 1-hour peptide treatment, as mentioned before (Section 3.6.2.). Samples were then analyzed using confocal microscopy.

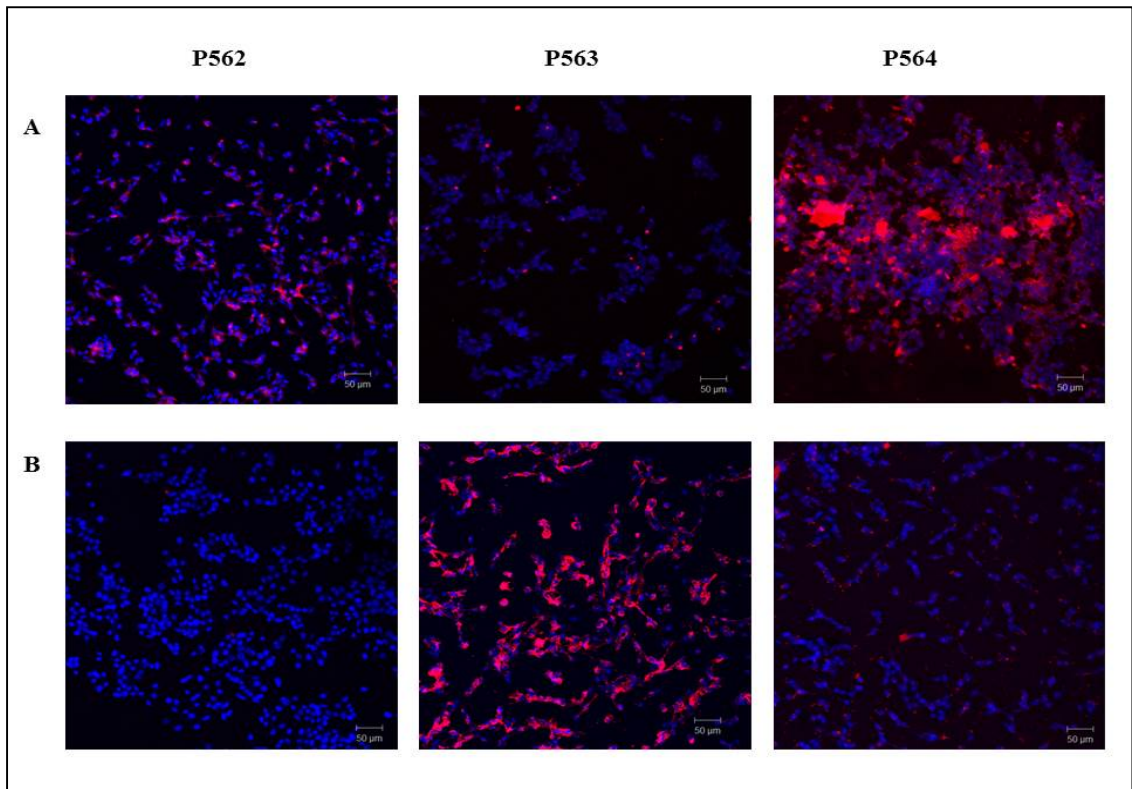


Figure 4.17. Peptide binding Affinity on **A.** PNT1A cell line **B.** 22RV1 cell line by confocal microscopy. Images were taken at 10X magnification. Bar, 50μm

Confocal imaging indicated that P562 fail to bind 22RV1 cells leastwise, bind to PNT1A . In contrast, P563 bind to the cancer cell line at high level besides very low binding was detected on PNT1A cells as shown at Figure 4.11. While TAMRA conjugated, P564 bind to PNT1A cells at high level. Red-stained cells showed the peptide binding cells and Blue stained cells shows DAPI which is the nuclear and chromosomal counterstain.

5. DISCUSSION

Prostate cancer is the second most frequently diagnosed cancer, which is about 15-20% of all male cancers worldwide. Within the group of men who died of cancer, prostate cancer causes about seven per cent of deaths, and thus represents the fourth most common lethal cancer after the lung, colorectal cancer, and breast cancer. [19] Mechanisms responsible for the formation and the progression of prostate cancer has not been completely discovered yet. [21] However, many different factors known as signal transduction pathways, changes in angiogenesis, and adhesion molecules are considered to have role in the prostate cancer. [23-24]

Since prostate cancer has a low survival rate, different combination and targeted therapies has been under investigation to achieve a successful treatment. Today, the most studied and promising approach in cancer treatment is to transport the active ingredients using nanoparticle drug delivery systems. [14] Various nano-carriers, including polymersomes and liposomes, have been used for this purpose. Thereby, the focus of this thesis is the development of gene therapy using Poly(2-ethyl-2-oxazoline) (PEtOx) as multifunctional carrier systems that can be targeted with peptide conjugations for the treatment of the Prostate cancer. [46-47]

Recent studies suggesting 22RV1 cells to be resistant to TRAIL-induced apoptosis, brought about the need for another pro-apoptotic gene to be selected for the present study. In that, 22RV1 cells transfected with TRAIL using commercially available transfection agents resulted in a 10 per cent apoptotic death, but the cell mortality could be increased up to 50 per cent when using the newly developed multifunctional nano-carriers. [71] Since the aim of the project is to use a novel pro-apoptotic gene that should have at least similar apoptotic, the newly generated mutant form of BIK gene, BIKDDA, which has been shown to induce cell death in breast cancer cell line, [37] was selected as the candidate pro-apoptotic gene for this thesis. In order to generate a more lethal form of BIK gene, Liu et al. first developed BIKDD and showed that it caused the destruction of cancer cells such as pancreatic, lung, and breast cancer cells. [73-74-75]. In the follow-up studies, BIKDDA gene, another phosphorylation mimic mutant form of the BIK protein with a longer life span and higher apoptosis-inducing effect than BIKDD gene, was used as pro-apoptotic

gene [77-79]. BIKDDA, binds and sterically blocks the function of anti-apoptotic Bcl-2 and Bcl-xL proteins, which in turn induces the mitochondrial outer membrane permeabilization. [72] Therefore to start with, we have compared the lethality of TRAIL and BIKDDA expression in 22RV1 cell line. Our results showed that BIKDDA was successfully expressed in 22RV1 in time-dependent manner. Similarly, Jiao *et al.* (2014) found that the expression of BIK gene was increased in time dependent manner in estrogen independent cell line MDA-MB-231. [58] TRAIL expression on TRAIL transfected 22RV1 cells was found to peak at 48 hours. However, Gravina *et al.* 2016 showed the expression of TRAIL gene in 22RV1 cells to increase gradually within 96 hours.

In order to determine the comparative lethal effect of pro-apoptotic BIKDDA and TRAIL genes on 22RV1 cells, trypan blue assay was done to analyze the percentage of the cell viability. Transfection of 22RV1 cells with BIKDDA resulted in 60-70 per cent cell death within 72 hours, while TRAIL transfection only induced 30-50 per cent death within the given time frame suggesting that BIKDDA is a better pro-apoptotic gene to be used as gene therapy agent for the treatment of prostate cancer. Our results were consistent with the literature showing that 22RV1 cells underwent 30-50 per cent cell death when transfected by the TRAIL gene [37].

In order to confirm our results, Annexin V staining was performed to detect apoptosis rate. Consistent with the trypan blue data, BIKDDA transfected 22RV1 cells exhibited around 40 per cent cell death at 24 hours, while the off-target effects of backbone plasmid was eliminated. Since there was no remarkable cell death was detected when 22RV1 cells were transfected with peGFPC3. We concluded that the pro-apoptotic gene, BIKDDA has higher lethal effect on 22RV1 cells in comparison with TRAIL. [59]

PEtOx-co-PEI polymer is more advantageous than any other polymers in the literature in terms of biocompatibility and cellular interaction, stealth effect, and availability for functionality. [74] The use of PEtOx was approved by the FDA not only as an indirect food supplement but also as drug carrier, thus the use of biomaterials based on PEtOx is expected to grow rapidly.[75] Pioneer study demonstrated that, PEtOx-b-PCL and PEtOx PLA polymers could be used as polymer therapeutics as they possess no cytotoxic effect on human dermal fibroblasts and liver hepatocellular cells.[63] In light of these findings, this current study focused on the use of PetOx5900-b-PCL4200 as the nano-carrier.

The cytotoxicity of polymersome polymer and formulation were evaluated under *in vitro* conditions. For that reason, four different cell types were used to investigate the cytotoxic effect of PEtOx-based polymer on the prostate epithelial, liver hepatocellular, human dermal fibroblast, and human fetal osteoblastic 1.19 cells. Treatment of the healthy prostate epithelial cell line PNT1A with polymersome polymer and formulation revealed no significant cytotoxicity, instead the cell proliferation rate of PNT1A cells was significantly increased once exposed to this polymer. On the other hand, PetOx5900-b-PCL4200 revealed a moderate toxicity in HEPG2 cell line. In contrast, studies show that there is non-cytotoxic effect of PetOx based nanocarriers on HEPG2 cells [77]. In agreement with the literature [64], treatment of the osteoblasts and HDFs with the PetOx based polymersome did not cause any significant change in the percentage of viable cells. According to the study conducted by Luxenhofer et al., the cytotoxicity of Poly(2-oxazoline) on healthy and cancer cells could be changed due to their chemical and physical properties. Given our results showing that PetOx5900-b-PCL4200 polymersome did not cause significant toxicity to healthy human cells, this polymer can be used as a drug-carrier. [77]

The prostate-specific-membrane antigen (PSMA), which was first discovered in 1997 by Kawakami et al. is overexpressed in prostate cancer. [82] Shen et al. their group developed high affinity peptide sequences recognizing PSMA and suggested that these peptides could be useful in the targeting nanoparticles used in drug delivery systems [83] In addition, Agarwal *et al.* proposed that small peptides selectively binding to PSMA producing cells may be used for the selective delivery of drugs to the malignant sites as an alternative to antibody-based anti-PSMA therapies. [84] According to the literature, fluorescently labeled PMSA-specific dimeric peptides did not show significant binding to PSMA-negative cells such as PC-3 and DU-145, while these peptides specifically bind to PSMA-positive prostate cancer cells such as LNCaP and CWR22R *in vitro* conditions. Similarly, within the scope of this study, prostate membrane specific antigen (PMSA) binding peptides such as peptide 562, 563 or 564 was intended to be used for the targeting prostate cancer [86]. Flow cytometry and confocal microscopy results indicated that among the three peptides tested, Peptide 563 was the only one that displayed low binding ability to the healthy control cell lines PNT1A and HUVEC, while it showed a high binding affinity towards 22RV1, suggesting that this peptide can be used in the targeting of BIKDDA

encapsulated PetOx5900-b-PCL4200 polymersomes to the PMSA-positive prostate cancer cells such as 22RV1.

In conclusion, this study aimed to develop a new gene therapy approach to specifically target prostate cancer using new generation nano-carrier system delivering a pro-apoptotic gene, BIKDDA which has not been used in the treatment of prostate cancer before. For this purpose, a Poly(2-ethyl-2-oxazoline) (PEtOx) based multifunctional carrier systems was used to prepare polymersome nanoparticles carrying the BIKDDA gene. To specifically target the prostate cancer, a comparative study between healthy and prostate cancer cell lines was performed using PMSA-targeting peptides to determine the most effective peptide that recognizes PMSA antigen. In this study, the effect of BIKDDA carrying polymersome on cell viability were analyzed by flow cytometry and it was found that PsM-BIKDDA is the effective carrier system and have role in inducing apoptosis. In addition, peptides which recognizes PSMA antigen was used and according to the results, peptide 563 had the ability to bind specifically prostate cancer cells.

6. FUTURE PROSPECTS

For further studies, it is important to reveal the targeting efficiency of P563 loaded polymersomes on 22RV1 cell line. In addition, chemotherapeutic agent such as Docetaxel can be used to load P563 targeted polymersomes to apoptosis specifically in PMSA-positive prostate cancer cells. Lastly, *in vivo* tests can be done with the P563-targeted polymersomes delivering pro-apoptotic genes or chemotherapeutic agents to xenograph tumor models developed using PSMA-positive cells.

As a result of this study, we foresee a brilliant future for the development of polymersomes as drug delivery vehicles that can be potentially used as diagnostic and therapeutic agents. In particular, we believe that the use of strategies to maximize clinical compliance will play an important role in the development of functional polymersomes that are useful for future therapeutic applications.

The future prospects of the project also include optimized and *in-vivo* tested nano-vehicle formulations that can be produced in the GMP laboratories provided that prior knowledge about scale-up is obtained by the evaluation the effect of critical process and formulation parameters on the final product.

REFERENCES

1. R. S. Kirby. Anatomy and Pathophysiology of the Prostate Gland. *Epidemiology of Prostate Disease*, pages 3-12. Springer Berlin Heidelberg, Berlin, Heidelberg, 1995.
2. A. Bhavsar and S. Verma. Anatomic Imaging of the Prostate. *BioMed Research International*, 2014:9, 2014.
3. R. Greenhalgh and R. S. Kirby. Anatomy and Physiology of the Prostate and Benign Prostatic Hyperplasia. *Atlas of the Urologic Clinics of North America*, 10:1-9, 1990.
4. L. Costello and R. Franklin. Prostatic Fluid Electrolyte Composition for the Screening of Prostate Cancer: a Potential Solution to a Major Problem. *Prostate Cancer Prostatic Diseases*, 12:17-24, 2009.
5. G. Sahlén, O. Nilsson, A. Larsson, L. Carlsson, B. J. Norlén and G. Ronquist. Secretions from Seminal Vesicles Lack Characteristic Markers for Prostatasomes. *Upsala Journal of Medical Sciences*, 115:107-112, 2010.
6. P. Kumar, N. Kumar, D. S. Thakur and A. Patidar. Male hypogonadism: Symptoms and Treatment. *Journal of Advanced Pharmaceutical Technology and Research*, 1:297-301, 2010.
7. J. Kurhanewicz, D. B. Vigneron, R. G. Males, M. G. Swanson, K. K. Yu and H. Hricak. The Prostate: Mr Imaging and Spectroscopy. *Radiologic Clinics*, 38:115-138, 2000.
8. V. J. Sharp, E. B. Takacs and C. R. Powell. Prostatitis: Diagnosis and Treatment. *American Academy of Family Physicians*, 82:397-406, 2010.
9. S. J. Berry, D. S. Coffey, P. C. Walsh and L. L. Ewing. The Development of Human Benign Prostatic Hyperplasia with Age. *The Journal of Urology*, 132:474-479, 1984.

10. L. Bubendorf, M. Kolmer, J. Kononen, P. Koivisto, S. Mousses, Y. Chen, E. Mahlamäki, P. Schraml, H. Moch, N. Willi, A. G. Elkahloun, T. G. Pretlow, T. C. Gasser, M. J. Mihatsch, G. Sauter and O.P. Kallioniemi. Hormone Therapy Failure in Human Prostate Cancer: Analysis by Complementary DNA and Tissue Microarrays. *Journal of the National Cancer Institute*, 91:1758-1764, 1999.
11. W. A. Schulz, M. Burchardt and M. V. Cronauer. Molecular Biology of Prostate Cancer. *Molecular Human Reproduction*, 9:437-448, 2003.
12. R. Siegel, D. Naishadham and A. Jemal. Cancer Statistics, 2012. *A Cancer Journal for Clinicians*, 62:10-29, 2012.
13. A. Partin, J. Yoo, H. B. Carter, J. Pearson, D. Chan, J. Epstein and P. Walsh. The Use of Prostate Specific Antigen, Clinical Stage and Gleason Score to Predict Pathological Stage in Men with Localized Prostate Cancer. *The Journal of Urology*, 150:110-114, 1993.
14. J. Rotow, S. R. Gameiro, R. A. Madan, J. L. Gulley, J. Schlom and J. W. Hodge. Vaccines as Monotherapy and in Combination Therapy for Prostate Cancer. *Clinical and Translational Science*, 3:116-122, 2010.
15. J. W. Hodge, A. Ardiani, B. Farsaci, A. R. Kwilas and S. Gameiro. The Tipping Point for Combination Therapy: Cancer Vaccines with Radiation, Chemotherapy, or Targeted Small Molecule Inhibitors. *Seminars in Oncology*, 39:323-339, 2012.
16. S. M. Dhanasekaran, T. R. Barrette, D. Ghosh, R. Shah, S. Varambally, K. Kurachi, K. J. Pienta, M. A. Rubin and A. M. Chinnaiyan. Delineation of Prognostic Biomarkers in Prostate Cancer. *Nature*, 412:822-826, 2001.
17. L. A. Kraus, S. K. Samuel, S. M. Schmid, D. J. Dykes, W. R. Waud and M. C. Bissery. The Mechanism of Action of Docetaxel (Taxotere®) in Xenograft models is not Limited to Bcl-2 Phosphorylation. *Investigational New Drugs*, 21:259-268, 2003.

18. B. Dahllöf, A. Billström, F. Cabral and B. Hartley Asp. Estramustine Depolymerizes Microtubules by Binding to Tubulin. *Cancer Research*, 53:4573-4581, 1993.
19. G. Chodak. Prostate Cancer: Epidemiology, Screening, and Biomarkers. *Nature Reviews in Urology*, 8:3-8, 2006.
20. G. P. Haas, N. Delongchamps, O. W. Brawley, C. Y. Wang and G. de la Roza. The Worldwide Epidemiology of Prostate Cancer: Perspectives from Autopsy Studies. *Canadian Journal of Urology*, 15:3866-3871, 2008.
21. F. Galtier. Definition, Epidemiology, Risk Factors. *Diabetes Metab*, 36:628-651, 2010.
22. D. Stasiewicz, E. Staroslawska, A. Brzozowska, A. Mocarska, M. Losicki, J. Szumilo and F. Burdan. Epidemiology and Risk Factors of the Prostate Cancer. *Polski Merkurusz Lekarski*, 33:163-167, 2012.
23. P. H. Gann. Risk Factors for Prostate Cancer. *Nature Reviews in Urology*, 4:3-10, 2002.
24. F. Menegaux, A. Anger, H. Randrianasolo, C. Mulot, P. Laurent-Puig, F. Iborra, J.-P. Bringer, B. Leizour, R. Thuret, P.J. Lamy, X. Rébillard and B. Trétarre. Epidemiological Study of Prostate Cancer (EPICAP): A Population-Based Case–Control Study in France. *BMC Cancer*, 14:106, 2014.
25. L. F. Diaz, M. Chiong, A. F. G. Quest, S. Lavandero and A. Stutzin. Mechanisms of Cell Death: Molecular Insights and Therapeutic Perspectives. *Cell Death and Differentiation*, 12:1449-1456, 2005.
26. S. Elmore. Apoptosis: A Review of Programmed Cell Death. *Toxicologic Pathology*, 35:495-516, 2007.
27. S. Fulda and K. M. Debatin. Extrinsic Versus Intrinsic Apoptosis Pathways in Anticancer Chemotherapy. *Oncogene*, 25:4798-4811, 2000.

28. M. H. Cardone, N. Roy, H. R. Stennicke, G. S. Salvesen, T. F. Franke, E. Stanbridge, S. Frisch and J. C. Reed. Regulation of Cell Death Protease Caspase-9 by Phosphorylation. *Science*, 282:1318-1321, 1998.
29. D. R. Green and G. Kroemer. The Pathophysiology of Mitochondrial Cell Death. *Science*, 305:626-629, 2004.
30. D. Hanahan and R. A. Weinberg. The Hallmarks of Cancer. *Cell*, 100:57-70, 2000.
31. R. J. Youle and A. Strasser. The BCL-2 Protein Family: Opposing Activities that Mediate Cell Death. *Nature Reviews of Molecular Cell Biology*, 9:47-59, 2008.
32. B. J. Feldman and D. Feldman. The Development of Androgen-Independent Prostate Cancer. *Nature Reviews of Cancers*, 1:34-45, 2001.
33. K. J. Pienta and D. Bradley. Mechanisms Underlying the Development of Androgen-Independent Prostate Cancer. *Clinical Cancer Research*, 12:1665-1671, 2006.
34. M.E. Taplin and S. P. Balk. Androgen Receptor: A Key Molecule in the Progression of Prostate Cancer to Hormone Independence. *Journal of Cellular Biochemistry*, 91:483-190, 2004.
35. J. R. Gingrich, R. J. Barrios, R. A. Morton, B. F. Boyce, F. J. DeMayo, M. J. Finegold, R. Angelopoulou, J. M. Rosen and N. M. Greenberg. Metastatic Prostate Cancer in a Transgenic Mouse. *Cancer Research*, 56:4096-4102, 1996.
36. J. Li, C. Yen, D. Liaw, K. Podsypanina, S. Bose, S. I. Wang, J. Puc, C. Miliareisis, L. Rodgers, R. McCombie, S. H. Bigner, B. C. Giovanella, M. Ittmann, B. Tycko, H. Hibshoosh, M. H. Wigler and R. Parsons. A Putative Protein Tyrosine Phosphatase Gene Mutated in Human Brain, Breast, and Prostate Cancer. *Science*, 275:1943-1947, 1997.

37. A. D. Sanlioglu, I. T. Koksall, B. Karacay, M. Baykara, G. Luleci and S. Sanlioglu. Adenovirus-Mediated Expression Sensitizes Prostate Carcinoma Cells to TRAIL-Induced Apoptosis. *Cancer Gene Therapy*, 13:21-31, 2005.
38. J. Carpten, N. Nupponen, S. Isaacs, R. Sood, C. Robbins, J. Xu, M. Faruque, T. Moses, C. Ewing, E. Gillanders, P. Hu, P. Bujnovszky, I. Makalowska, A. Baffoe Bonnie, D. Faith, J. Smith, D. Stephan, K. Wiley, M. Brownstein, D. Gildea, B. Kelly, R. Jenkins, G. Hostetter, M. Matikainen, J. Schleutker, K. Klinger, T. Connors, Y. Xiang, Z. Wang and A. De Marzo. Germline Mutations in the Ribonuclease L Gene in Families Showing Linkage with HPC1. *Nature Genetics*, 30, 2002.
39. A. Thibault, W. D. Figg, R. C. Bergan, R. M. Lush, C. E. Myers, A. Tompkins, E. Reed and D. Samid. A Phase II Study of 5-Aza-2'deoxyctidine (Decitabine) in Hormone Independent Metastatic (D2) Prostate Cancer. *Tumori*, 84:87-89, 1998.
40. J. Ghosh and C. E. Myers. Inhibition of Arachidonate 5-Lipoxygenase Triggers Massive Apoptosis in Human Prostate Cancer Cells. *Proceedings of the National Academy of Sciences*, 95:13182-13187, 1998.
41. E. D. Crawford, M. Rosenblum, A. M. Ziada and P. H. Lange. Overview: Hormone Refractory Prostate Cancer. *Urology*, 54:1-7, 2000.
42. I. U. Ali, L. M. Schriml and M. Dean. Mutational Spectra of PTEN/MMAC1 Gene: a Tumor Suppressor With Lipid Phosphatase Activity. *Journal of the National Cancer Institute*, 91:1922-1932, 1999.
43. G. J. Kelloff, J. A. Crowell, V. E. Steele, R. A. Lubet, C. W. Boone, W. A. Malone, E. T. Hawk, R. Lieberman, J. A. Lawrence, L. Kopelovich, I. Ali, J. L. Viner and C. C. Sigman. Progress in Cancer Chemoprevention. *Annals of the New York Academy of Sciences*, 889:1-13, 1999.

44. M. Roy, H. J. Kung and P. M. Ghosh. Statins and Prostate Cancer: Role of Cholesterol Inhibition vs. Prevention of Small GTP-Binding Proteins. *American Journal of Cancer Research*, 1:542-561, 2011.
45. B. H. Jiang and L. Z. Liu. PI3K/PTEN Signaling in Angiogenesis and Tumorigenesis. *Advanced Cancer Research*, 102:19-65, 2009.
46. P. Liu, H. Cheng, T. M. Roberts and J. J. Zhao. Targeting the Phosphoinositide 3-Kinase (PI3K) Pathway in Cancer. *Nature Reviews Drug Discovery*, 8:627-644, 2009.
47. J. LoPiccolo, G. M. Blumenthal, W. B. Bernstein and P. A. Dennis. Targeting the PI3K/Akt/mTOR Pathway: Effective Combinations and Clinical Considerations. *Drug Resistance Updates*, 11:32-50, 2008.
48. A. Sekulić, C. C. Hudson, J. L. Homme, P. Yin, D. M. Otterness, L. M. Karnitz and R. T. Abraham. A Direct Linkage between the Phosphoinositide 3-Kinase-AKT Signaling Pathway and the Mammalian Target of Rapamycin in Mitogen-stimulated and Transformed Cells. *Cancer Research*, 60:3504-3513, 2000.
49. T. L. Yuan and L. C. Cantley. PI3K Pathway Alterations in Cancer: Variations on a Theme. *Oncogene*, 27:5497-5510, 2008.
50. T. M. Morgan, T. D. Koreckij and E. Corey. Targeted Therapy for Advanced Prostate Cancer: Inhibition of the PI3K/Akt/mTOR Pathway. *Current Cancer Drug Targets*, 9:237-249, 2009.
51. N. T. Ihle, R. Lemos, P. Wipf, A. Yacoub, C. Mitchell, D. Siwak, G. B. Mills, P. Dent, D. L. Kirkpatrick and G. Powis. Mutations in the Phosphatidylinositol-3-Kinase Pathway Predict for Antitumor Activity of the Inhibitor PX-866 whereas Oncogenic Ras is a Dominant Predictor for Resistance. *Cancer Research*, 69:143-150, 2009.
52. B. D. Manning and L. C. Cantley. AKT/PKB Signaling: Navigating Downstream. *Cell*, 129:1261-1274, 2007.

53. S. Phin, M. W. Moore and P. D. Cotter. Genomic Rearrangements of PTEN in Prostate Cancer. *Frontiers in Oncology*, 3, 2013.
54. M. Yoshimoto, A. M. Joshua, I. W. Cunha, R. A. Coudry, F. P. Fonseca, O. Ludkovski, M. Zielenska, F. A. Soares and J. A. Squire. Absence of TMPRSS2:ERG Fusions and PTEN Losses in Prostate Cancer is Associated with a Favorable Outcome. *Modern Pathology*, 21:1451-1460, 2008.
55. M. Yoshimoto, I. W. Cunha, R. A. Coudry, F. P. Fonseca, C. H. Torres, F. A. Soares and J. A. Squire. FISH Analysis of 107 Prostate Cancers Shows that PTEN Genomic Deletion is Associated with Poor Clinical Outcome. *British Journal of Cancer*, 97:678-685, 2007.
56. K. Sircar, M. Yoshimoto, F. A. Monzon, I. H. Koumakpayi, R. L. Katz, A. Khanna, K. Alvarez, G. Chen, A. D. Darnel, A. G. Aprikian, F. Saad, T. A. Bismar and J. A. Squire. PTEN Genomic Deletion is Associated with P-Akt And AR Signalling in Poorer Outcome, Hormone Refractory Prostate Cancer. *Journal of Pathology*, 218:505-513, 2009.
57. X. Xie, Y. Kong, H. Tang, L. Yang, J. L. Hsu and M. C. Hung. Targeted Bikdd Expression Kills Androgen-Dependent and Castration-Resistant Prostate Cancer Cells. *Molecular Cancer Therapeutics*, 13:1813-1825, 2014.
58. Y. Sun, M. Ponz-Sarvise, S. S. Chang, W. C. Chang, C. H. Chen, J. L. Hsu and M. C. Hung. Proteasome Inhibition Enhances the Killing Effect of Bikdd Gene Therapy. *American Journal of Translational Research*, 7:319-327, 2015.
59. V. Pandya, D. Glubrecht, L. Vos, J. Hanson, S. Damaraju, J. Mackey, J. Hugh and I. S. Goping. The Pro-Apoptotic Paradox: The BH3-Only Protein Bcl-2 Interacting Killer (Bik) is Prognostic for Unfavorable Outcomes in Breast Cancer. *Oncotarget*, 7:33272-33285, 2016.

60. S. Jiao, M. Wu, F. Ye, H. Tang, and X. Xie. BikDDA, A Mutant of Bik with Longer Half-Life Expression Protein, can be a Novel Therapeutic Gene for Triple-Negative Breast Cancer. *PLoS One*, 9:9_2-17_2, 2014.
61. F. H. Schröder, P. Hermanek, L. Denis, W. R. Fair, M. K. Gospodarowicz and M. Pavone-Macaluso. The TNM Classification of Prostate Cancer. *The Prostate*, 21:129-138, 1992.
62. W. Jiang, M. Puntis and M. Hallett. Molecular and Cellular Basis of Cancer Invasion and Metastasis: Implications for Treatment. *British Journal of Surgery*, 81:1576-1590, 1994.
63. T. N. Stitt, D. Drujan, B. A. Clarke, F. Panaro, Y. Timofeyva, W. O. Kline, M. Gonzalez, G. D. Yancopoulos and D. J. Glass. The IGF-1/PI3K/Akt Pathway Prevents Expression of Muscle Atrophy-Induced Ubiquitin Ligases by Inhibiting FOXO Transcription Factors. *Molecular Cell*, 14:395-403, 2004.
64. A. J. Levine, Z. Feng, T. W. Mak, H. You and S. Jin. Coordination and Communication Between the P53 And IGF-1–AKT–TOR Signal Transduction Pathways. *Genes & Development*, 20:267-275, 2006.
65. G. O. Hellawell, G. D. Turner, D. R. Davies, R. Poulson, S. F. Brewster and V. M. Macaulay. Expression of the Type 1 Insulin-Like Growth Factor Receptor is Up-Regulated in Primary Prostate Cancer and Commonly Persists in Metastatic Disease. *Cancer Research*, 62:2942-2950, 2002.
66. A. A. Samani, S. Yakar, D. LeRoith and P. Brodt. The Role of the IGF System in Cancer Growth and Metastasis: Overview and Recent Insights. *Endocrine Reviews*, 28:20-47, 2007.
67. F. A. Ferrer, L. J. Miller, R. I. Andrawis, S. H. Kurtzman, P. C. Albertsen, V. P. Laudone and D. L. Kreutzer. Vascular Endothelial Growth Factor (VEGF) Expression in

Human Prostate Cancer: In Situ And In Vitro Expression of VEGF by Human Prostate Cancer Cells. *The Journal of Urology*, 157:2329-2333, 1997.

68. R. Mazzucchelli, R. Montironi, A. Santinelli, G. Lucarini, A. Pignatelli and G. Biagini. Vascular Endothelial Growth Factor Expression and Capillary Architecture in High-Grade PIN and Prostate Cancer in Untreated and Androgen-Ablated Patients. *The Prostate*, 45:72-79, 2000.

69. J. Plati, O. Bucur and R. Khosravi-Far. Apoptotic Cell Signaling in Cancer Progression and Therapy. *Integrative Biology*, 3:279-296, 2011.

70. K. M. Boatright and G. S. Salvesen. Mechanisms of Caspase Activation. *Current Opinion in Cell Biology*, 15:725-731, 2003.

71. N. Maherali, R. Sridharan, W. Xie, J. Utikal, S. Eminli, K. Arnold, M. Stadtfeld, R. Yachechko, J. Tchieu and R. Jaenisch. Directly Reprogrammed Fibroblasts Show Global Epigenetic Remodeling and Widespread Tissue Contribution. *Cell Stem Cell*, 1:55-70, 2007.

72. J.-Y. Lang, J. L. Hsu, F. Meric-Bernstam, C.-J. Chang, Q. Wang, Y. Bao, H. Yamaguchi, X. Xie, W. A. Woodward and D. Yu. BikDD Eliminates Breast Cancer Initiating Cells and Synergizes with Lapatinib for Breast Cancer Treatment. *Cancer Cell*, 20:341-356, 2011.

73. O. C. Farokhzad, S. Jon, A. Khademhosseini, T. N. T. Tran, D. A. LaVan and R. Langer. Nanoparticle-Aptamer Bioconjugates a New Approach for Targeting Prostate Cancer Cells. *Cancer Research*, 64:7668-7672, 2004.

74. D. H. Levine, P. P. Ghoroghchian, J. Freudenberg, G. Zhang, M. J. Therien, M. I. Greene, D. A. Hammer and R. Murali. Polymersomes: a New Multi-Functional Tool for Cancer Diagnosis and Therapy. *Methods*, 46:25-32, 2008.

75. K. Cho, X. Wang, S. Nie and D. M. Shin. Therapeutic Nanoparticles for Drug Delivery in Cancer. *Clinical Cancer Research*, 14:1310-1316, 2008.
76. S. Maya, B. Sarmiento, A. Nair, N. S. Rejinold, S. V. Nair and R. Jayakumar. Smart Stimuli Sensitive Nanogels in Cancer Drug Delivery and Imaging: A Review. *Current Pharmaceutical Design*, 19:7203-7218, 2013.
77. R. Hoogenboom. Poly (2-oxazoline): a Polymer Class with Numerous Potential Applications. *Angewandte Chemie International Edition*, 48:7978-7994, 2009.
78. K. Knop, R. Hoogenboom, D. Fischer and U. S. Schubert. Poly (Ethylene Glycol) in Drug Delivery: Pros and Cons as well as Potential Alternatives. *Angewandte Chemie International Edition*, 49:6288-6308, 2010.
79. P. M. Peiris, L. Bauer, R. Toy, E. Tran, J. Pansky, E. Doolittle, E. Schmidt, E. Hayden, A. Mayer, R. A. Keri, M. A. Griswold and E. Karathanasis. Enhanced Delivery of Chemotherapy to Tumors Using a Multicomponent Nanochain with Radio-Frequency-Tunable Drug Release. *ACS Nano*, 6:4157-4168, 2012.
80. K. T. Kim, J. J. Cornelissen, R. J. Nolte and J. van Hest. A Polymersome Nanoreactor with Controllable Permeability Induced by Stimuli-Responsive Block Copolymers. *Advanced Materials*, 21:2787-2791, 2009.
81. X. Wu, B. Ding, J. Gao, H. Wang, W. Fan, X. Wang, W. Zhang, L. Ye, M. Zhang and X. Ding. Second-Generation Aptamer-Conjugated PSMA-Targeted Delivery System for Prostate Cancer Therapy. *International Journal of Nanomedicine*, 6:1747-1756, 2011.
82. S. R. Banerjee, M. Pullambhatla, Y. Byun, S. Nimmagadda, G. Green, J. J. Fox, A. Horti, R. C. Mease and M. G. Pomper. ⁶⁸Ga-Labeled Inhibitors of Prostate-Specific Membrane Antigen (PSMA) for Imaging Prostate Cancer. *Journal of Medicinal Chemistry*, 53:5333-5341, 2010.

83. B. Xiang, D.-W. Dong, N.-Q. Shi, W. Gao, Z.-Z. Yang, Y. Cui, D.-Y. Cao and X.-R. Qi. PSA-Responsive and PSMA-Mediated Multifunctional Liposomes for Targeted Therapy of Prostate Cancer. *Biomaterials*, 34:6976-6991, 2013.
84. S. Aggarwal, P. Singh, O. Topaloglu, J. T. Isaacs and S. R. Denmeade. A Dimeric Peptide that Binds Selectively to Prostate-Specific Membrane Antigen and Inhibits its Enzymatic Activity. *Cancer Research*, 66:9171-9177, 2006.
85. A. Telerman, R. Amson, M. Tuijnder and L. Susini. Compositions and Methods for the Treatment of Cancer. Google Patents, 2003.
86. W. Tai, R. S. Shukla, B. Qin, B. Li and K. Cheng. Development of a Peptide-Drug Conjugate for Prostate Cancer Therapy. *Molecular Pharmaceutics*, 8:901-912, 2011.
87. S. Shankar, X. Chen and R. K. Srivastava. Effects of Sequential Treatments with Chemotherapeutic Drugs Followed by TRAIL on Prostate Cancer in Vitro and in Vivo. *The Prostate*, 62:165-186, 2005.
88. P. B. Singh, C. Anele, E. Dalton, O. Barbouti, D. Stevens, P. Gurung, M. Arya, C. Jameson, A. Freeman and M. Emberton. Prostate Cancer Tumour Features on Template Prostate-Mapping Biopsies: Implications for Focal Therapy. *European Urology*, 66:12-19, 2014.
89. J. Nicolas, S. Mura, D. Brambilla, N. Mackiewicz and P. Couvreur. Design, functionalization Strategies and Biomedical Applications of Targeted Biodegradable/Biocompatible Polymer-Based Nanocarriers for Drug Delivery. *Chemical Society Reviews*, 42:1147-1235, 2013.
90. G. Gregoriadis, C. Swain, E. Wills and A. Tavill. Drug-Carrier Potential of Liposomes in Cancer Chemotherapy. *The Lancet*, 303:1313-1316, 1974.
91. A. Yagoda and D. Petrylak. Cytotoxic Chemotherapy for Advanced Hormone-Resistant Prostate Cancer. *Cancer*, 71:1098-1109, 1993.

92. A. V. Schally and A. Nagy. Cancer Chemotherapy Based on Targeting of Cytotoxic Peptide Conjugates to Their Receptors on Tumors. *European Journal of Endocrinology*, 141:1-14, 1999.
93. G. Murphy, C. Mettlin, H. Menck, D. Winchester and A. Davidson. National Patterns of Prostate Cancer Treatment by Radical Prostatectomy: Results of a Survey by the American College of Surgeons Commission on Cancer. *The Journal of Urology*, 152:1817-1819, 1994.
94. A. L. Burnett, G. Aus, E. D. Canby-Hagino, M. S. Cookson, A. V. D'Amico, R. R. Dmochowski, D. T. Eton, J. D. Forman, S. L. Goldenberg and J. Hernandez. Erectile Function Outcome Reporting After Clinically Localized Prostate Cancer Treatment. *The Journal of Urology*, 178:597-601, 2007.
95. C. Fleming, J. H. Wasson, P. C. Albertsen, M. J. Barry, J. E. Wennberg, T. Bubolz, C. C. Lindsay, B. Littenberg, A. B. Flood and G. L. Lu-Yao. A decision Analysis of Alternative Treatment Strategies for Clinically Localized Prostate Cancer. *The Journal of American Medical Association*, 269:2650-2658, 1993.
96. C. A. Heinlein and C. Chang. Androgen Receptor in Prostate Cancer. *Endocrine Reviews*, 25:276-308, 2004.
97. M. Haverinen, S. Passinen, H. Syväälä, S. Pasanen, T. Manninen and P. Tuohimaa. Heat Shock Protein 90 and The Nuclear Transport of Progesterone Receptor. *Springer*, 6:256-262, 2001.
98. R. Chmelar, G. Buchanan, E. F. Need, W. Tilley and N. M. Greenberg. Androgen Receptor Coregulators and Their Involvement in the Development and Progression of Prostate Cancer. *International Journal of Cancer*, 120:719-733, 2007.

99. A. Molina and A. Belldgrun. Novel Therapeutic Strategies for Castration Resistant Prostate Cancer: Inhibition of Persistent Androgen Production and Androgen Receptor Mediated Signaling. *The Journal of Urology*, 185:787-794, 2011.

100. K. S. Ross, H. B. Carter, J. D. Pearson and H. A. Guess. Comparative Efficiency of Prostate-Specific Antigen Screening Strategies for Prostate Cancer Detection. *The Journal of American Medical Association*, 284:1399-1405, 2000.